USGS
science for a changing world

Scanning Electron Microscope Images of Sand and Silt from the Early MIS4–MIS3 Roxana Silt, Phillips Bayou, Arkansas

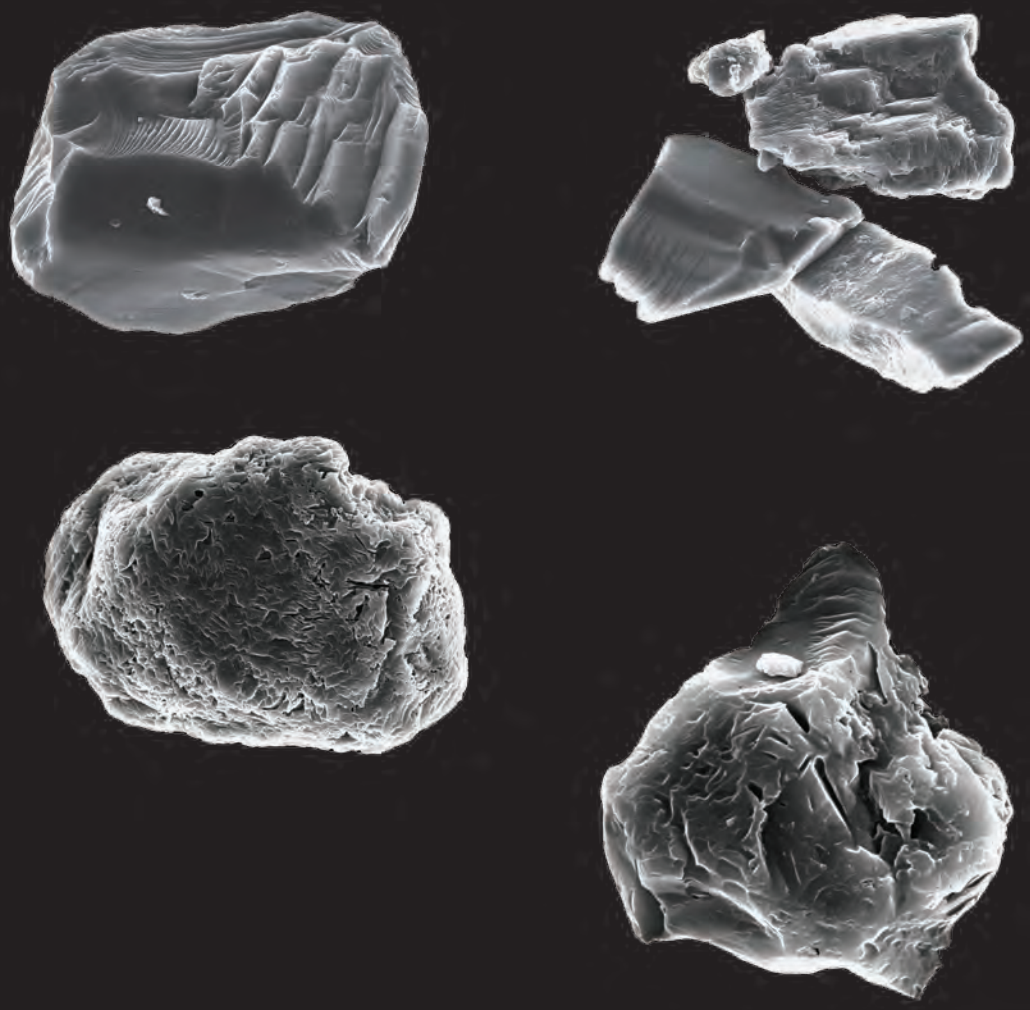

Scientific Investigations Report 2023–5062

U.S. Department of the Interior
U.S. Geological Survey

Cover. Scanning electron microscope images of grains from the Roxana Silt and Farmdale paleosol. Top and bottom left and top right images from unnamed paleosol in the lower part of the Roxana Silt; top left, quartz grain; top right, quartz and potassium feldspar grains; bottom left, potassium feldspar grain. Bottom right image is a plagioclase feldspar grain from the Farmdale paleosol. Scales vary.

Scanning Electron Microscope Images of Sand and Silt from the Early MIS4–MIS3 Roxana Silt, Phillips Bayou, Arkansas

Helaine W. Markewich, Douglas A. Wysocki, G. Norman White, and Joe B. Dixon

Scientific Investigations Report 2023–5062

U.S. Department of the Interior
U.S. Geological Survey

U.S. Geological Survey, Reston, Virginia: 2023

Suggested citation:
Markewich, H.W., Wysocki, D.A., White, G.N., and Dixon, J.B., Scanning electron microscope images of sand and silt from the early MIS4–MIS3 Roxana Silt, Phillips Bayou, Arkansas: U.S. Geological Survey Scientific Investigations Report 2023–5062, 24 p., https://doi.org/10.3133/sir20235062.

ISSN 2328-0328 (online)

Acknowledgments

Funding for the field work and for collection and analyses of laboratory samples was provided by the U.S. Geological Survey National Cooperative Geologic Mapping Program and Climate and Land-Use Change Research and Development Program. We thank Daniel R. Muhs, U.S. Geological Survey, and Marci Robinson, U.S. Geological Survey, for reviewing the manuscript.

Contents

Acknowledgments iii
Abstract 1
Introduction 1
Chronostratigraphy of Lower Mississippi Valley Eolian Silt Deposits 3
Roxana Silt Paleosol/Loess Chronostratigraphy at Phillips Bayou 5
SEM/EDS Investigations of the Roxana Silt at Phillips Bayou 10
Materials and Methods 10
Results of SEM/EDS Analysis 13
Summary of SEM/EDS analysis 19
Observations 20
References Cited 21

Figures

1. Partial maps of the United States showing major drainages within the Mississippi River drainage basin, approximate extent of loess distribution, approximate positions of Laurentide Ice Sheet glacial termini, and the study area in the lower Mississippi Valley 2
2. Chronostratigraphy of the Loveland Loess, Roxana Silt, Peoria Loess, and paleosols exposed in the cut-face of an inactive quarry near the former village of Phillips Bayou, Arkansas 4
3. Photograph of the quarry cut-face exposure near the former village of Phillips Bayou, Arkansas, showing contacts between the Loveland Loess, Roxana Silt, and Peoria Loess, and between the Farmdale paleosol and the unnamed paleosol in the Roxana Silt 7
4. Scanning electron microscope photograph of an iron oxide-coated sand-sized quartz grain from the unnamed paleosol in the lower part of the Roxana Silt, with a silt-sized iron oxide-coated potassium feldspar or muscovite grain on the quartz grain 12
5. Scanning electron microscope photographs of quartz sand grains and potassium feldspar sand grain from the unnamed paleosol in the lower part of the Roxana Silt 14
6. Scanning electron microscope photograph of rounded quartz sand from the unnamed paleosol in the lower part of the Roxana Silt 15
7. Scanning electron microscope photographs of quartz silt grain morphology from the Farmdale paleosol 15
8. Scanning electron microscope photographs of quartz silt grains with no visible depositional features from the Farmdale paleosol 16
9. Scanning electron microscope photographs of feldspar grain morphologies from the Farmdale paleosol, and the unnamed paleosol in the lower part of the Roxana Silt 17
10. Scanning electron microscope photographs of surface morphologies of pyroxenes and (or) amphiboles from 2A1 soil horizon, Farmdale paleosol 18
11. Scanning electron microscope photographs of titanium oxide morphologies from the Farmdale paleosol 19

12. Scanning electron microscope photograph of a muscovite sand grain from 2Bt4 soil horizon, Farmdale paleosol showing some delamination from weathering.....19

Tables

1. Timeline of loess deposition, paleosol development, and interpreted paleoclimate in the lower Mississippi Valley from northern Mississippi to east-central Missouri, southern Illinois, and southern Indiana.....5
2. Age data for the basal Peoria Loess and Roxana Silt exposed in the Phillips Bayou quarry cut-face near Phillips Bayou, Arkansas.....6
3. Paleosol/loess stratigraphy for the Roxana Silt section of the Phillips Bayou exposure as described by Ward and others, 1993.....8
4. Recognition criteria used for mineral identification for soil minerals observed by scanning electron microscopy/energy dispersive X-ray spectroscopy analysis.....11

Conversion Factors

U.S. customary units to International System of Units

Multiply	By	To obtain
	Length	
inch (in.)	2.54	centimeter (cm)
inch (in.)	25.4	millimeter (mm)
foot (ft)	0.3048	meter (m)
mile (mi)	1.609	kilometer (km)

International System of Units to U.S. customary units

Multiply	By	To obtain
	Length	
centimeter (cm)	0.3937	inch (in.)
millimeter (mm)	0.03937	inch (in.)
meter (m)	3.281	foot (ft)
kilometer (km)	0.6214	mile (mi)

Temperature in degrees Celsius (°C) may be converted to degrees Fahrenheit (°F) as follows:

$$°F = (1.8 \times °C) + 32.$$

Abbreviations

Au	gold
Ca	calcium
^{14}C	carbon-14
cm	centimeter
EDS	energy dispersive X-ray
Fe	iron
ka	kilo-annum (thousand years ago)
KSSL	Kellogg Soil Survey Laboratory
m	meter
MIS	marine isotope stage
MIS2	marine isotope stage 2
MIS3	marine isotope stage 3
MIS4	marine isotope stage 4
MIS5	marine isotope stage 5
MIS6	marine isotope stage 6
mm	millimeter
Mn	manganese
Na	sodium
SEM	scanning electron microscope
SEM/EDS	scanning electron microscopy/energy dispersive X-ray

Scanning Electron Microscope Images of Sand and Silt from the Early MIS4–MIS3 Roxana Silt, Phillips Bayou, Arkansas

Helaine W. Markewich[1], Douglas A. Wysocki[2], G. Norman White[3], and Joe B. Dixon[4]

Abstract

The age and source of the late Pleistocene Roxana Silt in the Mississippi Valley have been studied since the middle 1800s. Published age and paleoenvironmental data for the Roxana Silt in the Mississippi Valley show that deposition occurred from late marine isotope stage 5 (MIS5) through late marine isotope stage 3 (MIS3) (80–30 kilo-annum [ka]), when the warm to hot interglacial climate of early to middle MIS5 (about 130 to about 80 ka) was transitioning to a considerably cooler and wetter climate. Scanning electron microscopy/energy dispersive X-ray (SEM/EDS) analysis of silt and sand grains from the Roxana Silt exposed in an abandoned borrow pit near Phillips Bayou, Arkansas, was performed as part of a 1990s study of late middle and late Pleistocene loess in the unglaciated lower Mississippi Valley. Results from that study were summarized in 1990s publications, but the data for sand and silt grain morphology and mineralogy were not published. Some of the SEM/EDS analyses of the Roxana Silt from that late 1990s study are presented in this report. Combined with previously published chronostratigraphic and pedostratigraphic data for the Roxana Silt at Phillips Bayou, the SEM/EDS data indicate some degree of syndepositional weathering and pedogenic alteration during and after gradual eolian deposition in late marine isotope stage 4 (MIS4) and MIS3 (about 60 to about 30 ka). Results from the SEM/EDS analyses support previously published paleoclimate interpretations indicating that at least as far south as northern Mississippi, the climate of the Mississippi Valley in MIS4 and MIS3 (about 70 to about 30 ka) was cool to cold and humid to wet.

Introduction

The Mississippi River and its tributaries drain more than half the continental United States (fig. 1*A*). During the Pleistocene (from about 2.6 million to 12,000 years ago), the Laurentide Ice Sheet intermittently extended southward from Canada into the northern third of the Mississippi River basin. As the ice sheet retreated after each advance, glaciogenic deposits blanketed the land surface, including glacial till, glaciofluvial sand and gravel, slack water and lacustrine sediments, and eolian sand and silt. In large part, these deposits define the present landscape of the central United States and the northern part of the Mississippi Valley, including along and just south of the glacial limit (fig. 1*A*). In the unglaciated lower Mississippi Valley (area south of Thebes Gap on fig. 1*B*), glaciofluvial sediments and eolian silt are the dominant glaciogenic deposits. Full-glacial slack water or lacustrine deposits also are present, but exposures are limited (Rittenour and others, 2007, Grimley and others, 2009). Glaciofluvial sand and gravel form braided stream channel belts that are geomorphically expressed as terraces (Saucier, 1994; Rittenour and others, 2007). Eolian silt blankets many of the glaciofluvial terraces but also forms or caps high ridges within, and adjacent on the east to, the Mississippi Valley (fig. 1).

[1]U.S. Geological Survey, emeritus

[2]Natural Resources Conservation Service, emeritus

[3]Soil and Crop Sciences Department Texas A&M University, retired

[4]Soil and Crop Sciences Department Texas A&M University, deceased

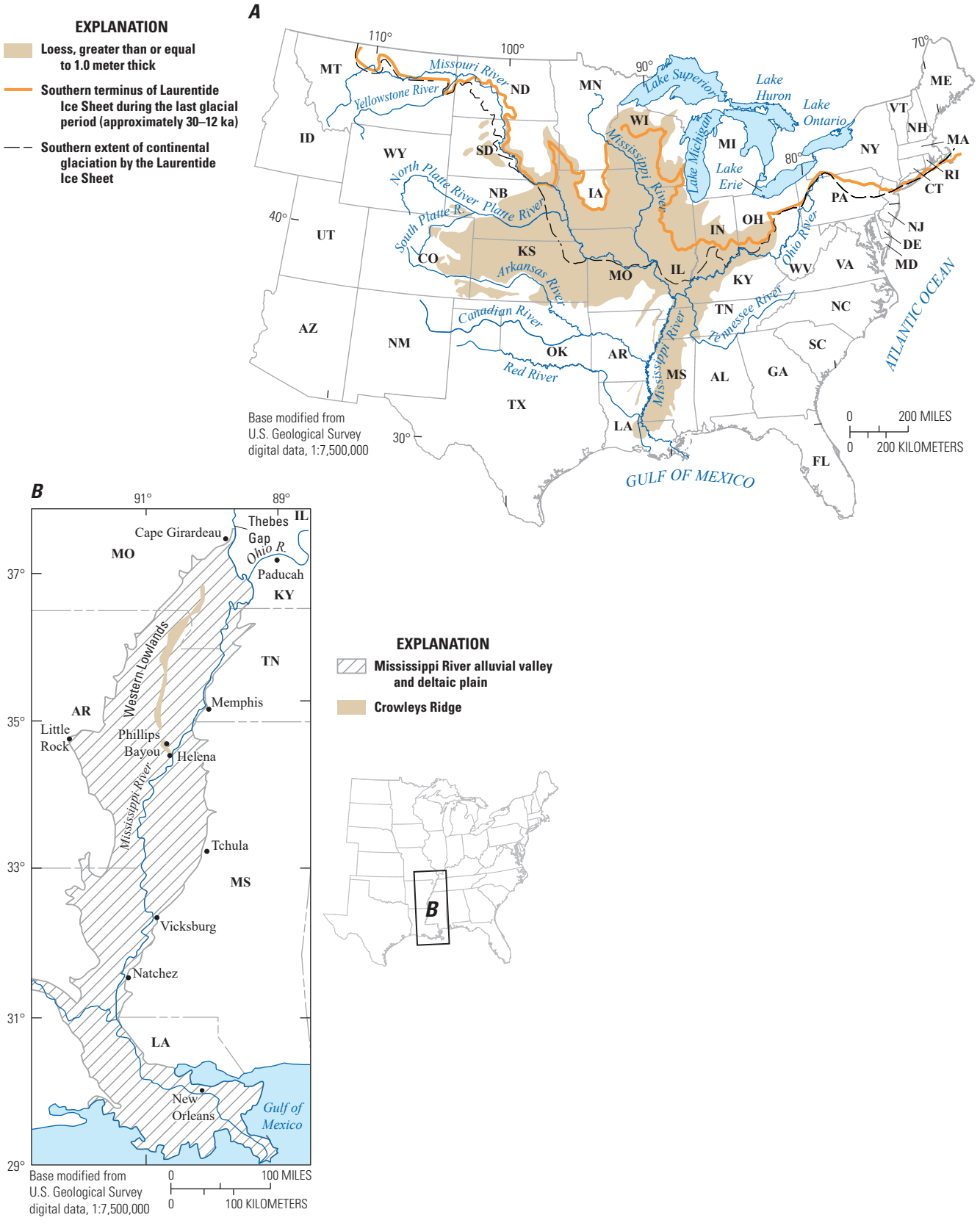
EXPLANATION
Loess, greater than or equal to 1.0 meter thick
Southern terminus of Laurentide Ice Sheet during the last glacial period (approximately 30–12 ka)
Southern extent of continental glaciation by the Laurentide Ice Sheet
A
110°
100°
90°
80°
70°
40°
30°
MT
ID
WY
UT
AZ
CO
NM
ND
SD
NB
KS
OK
TX
MN
IA
MO
AR
LA
WI
IL
MS
MI
IN
KY
TN
AL
OH
WV
GA
FL
SC
NC
VA
PA
NY
ME
VT
NH
MA
RI
CT
NJ
DE
MD
Missouri River
Yellowstone River
North Platte River
South Platte R.
Platte River
Arkansas River
Canadian River
Red River
Mississippi River
Ohio River
Tennessee River
Lake Superior
Lake Huron
Lake Michigan
Lake Ontario
Lake Erie
ATLANTIC OCEAN
GULF OF MEXICO
Base modified from U.S. Geological Survey digital data, 1:7,500,000
0 200 MILES
0 200 KILOMETERS
B
91°
89°
37°
35°
33°
31°
29°
MO
IL
KY
TN
AR
MS
LA
Cape Girardeau
Thebes Gap
Ohio R.
Paducah
Memphis
Little Rock
Phillips Bayou
Helena
Tchula
Vicksburg
Natchez
New Orleans
Gulf of Mexico
Western Lowlands
Mississippi River
EXPLANATION
Mississippi River alluvial valley and deltaic plain
Crowleys Ridge
B
Base modified from U.S. Geological Survey digital data, 1:7,500,000
0 100 MILES
0 100 KILOMETERS

Chronostratigraphy of Lower Mississippi Valley Eolian Silt Deposits

Although silt deposits in the lower Mississippi Valley were first discussed by Lyell (1847), there was no agreement on whether these deposits were windblown or water-lain until the 1950s and 1960s (see discussion and references in Follmer, 1996; Rutledge and others, 1996; and Markewich and others, 2011). By the 1970s, a windblown origin for these silt deposits generally had been accepted as the primary mode of deposition (see discussion and references in Follmer, 1996; Rutledge and others, 1996), but individual silt deposits containing gravity- or water-modified intervals were found to be common (McCraw and Autin, 1989; Rutledge and others, 1990; Jacobs and Knox, 1994; Leigh, 1994; Markewich and others, 2011) and locally difficult to distinguish from purely eolian silt deposits (loess). Numerous field investigations in the 1980s and 1990s focused on the origin, chronostratigraphy, and climatic significance of silt deposits in the unglaciated lower Mississippi Valley. These studies traced the stratigraphic sequence of loess deposits with increasing distance from the Laurentide Ice Sheet glacial margin by looking for continuous or discontinuous deposits (fig. 1). For example, Alford and Miller (1985), Miller and Alford (1985), Miller and others (1985), and Pye and Johnson (1988) suggested that some loesses older than the Peoria Loess (fig. 2) were eroded or never deposited in the southernmost part of the Mississippi Valley from west-central Mississippi to Louisiana (fig. 1), and that other loesses were present only in the southernmost part of the valley.

Most investigations of loess chronostratigraphy in the central United States and the Mississippi Valley during the 1980s and 1990s utilized new or advancing isotopic and luminescence dating methods. Methods that were being used in the 1980s and 1990s to date loess in the lower Mississippi Valley included thermoluminescence analyses (Huntley and others, 1985; Pye and Johnson, 1988; Forman, 1989; Rodbell and others, 1997; Markewich and others, 1998b), amino-acid racemization of mollusks found in the loess (Miller and others, 1988; Clark and others, 1989; McCoy and others, 1990; Mirecki and Miller, 1994), electron spin resonance (Mirecki and Skinner, 1991; Skinner and Mirecki, 1993), and cosmogenic beryllium-10 (^{10}B) analysis (Pavich and others, 1984; Pavich, 1993). Methods for dating organic material from loess deposits by radiocarbon (^{14}C) analysis were also advancing, and proportional gas counting and accelerator mass spectrometer ^{14}C analyses were also being applied to date organic material in loess (Rubin and others, 1993).

Chronostratigraphic data from the field investigations in the 1980s and 1990s indicated that the established late-middle Pleistocene and late Pleistocene loess stratigraphy of the central United States and northern Mississippi Valley could be extended into the lower Mississippi Valley as far south as west-central Mississippi and that age data were sufficient to correlate individual loess units with oxygen isotope stages and (or) marine isotope stages (fig. 1; Guccione and Rutledge, 1990; Follmer, 1996; Rutledge and others, 1996; Rodbell and others, 1997; Markewich and others, 1998b). From oldest to youngest, this loess stratigraphic sequence (fig. 2) is the Loveland Loess (MIS6, from about 185 ka to about 125 ka), Roxana Silt (MIS4, from about 70 ka to about 60 ka and MIS3, from about 60 to about 30 ka), and Peoria Loess (MIS2, from about 30 ka to about 12 ka) (age ranges for the marine isotope stages based on the LR04 stack in Railsback and others, 2015).

In the lower Mississippi Valley, the Loveland Loess and Roxana Silt each have at least one stratigraphically significant paleosol (fig. 2). The Sangamon paleosol, with its distinct yellow-red hue, high chroma colors (for example, 7.5*YR* 5/4 and 5/6), and well-developed pedologic structure, characterizes the upper part of the Loveland Loess. The Farmdale paleosol, with its much less red hue, lower chroma colors (for example, 10*YR* 4/3 and 4/4), and weak pedologic structure, characterizes the upper part of the Roxana Silt. Commonly, an unnamed paleosol is present in the lower part of the Roxana Silt and is superjacent to the Loveland Loess. The Sangamon paleosol, the unnamed paleosol, and the Farmdale paleosol are aggradational paleosols that formed during alternating periods of loess deposition and pedogenesis (Wang and others, 2009; Markewich and others, 2011). Table 1 shows a timeline summary for loess deposition and paleosol development in the lower Mississippi Valley that reached as far south as west-central Mississippi.

Figure 1. Maps of the study area. *A*, Map of the United States east of 117° W. longitude showing the major drainages within the Mississippi River drainage basin, approximate extent of loess distribution in the basin (modified from Thorp and others, 1952 and Muhs and others, 2018), and approximate positions of Laurentide Ice Sheet glacial termini east of 112° W. longitude. *B*, Map of the lower Mississippi Valley showing the location of geographic features and towns mentioned in this report and cities or towns that are not mentioned in this report but provide geographic context (for example, Vicksburg, Mississippi, and New Orleans, Louisiana). ka, thousand years ago; state abbreviations: AL, Alabama; AR, Arkansas; AZ, Arizona; CO, Colorado; CT, Connecticut; DE, Delaware; GA, Georgia; IA, Iowa; ID, Idaho; IL, Illinois; IN, Indiana; KS, Kansas; KY, Kentucky; LA, Louisiana; MA, Massachusetts; MD, Maryland; ME, Maine; MI, Michigan; MN, Minnesota; MO, Missouri; MS, Mississippi; MT, Montana; NM, New Mexico; NE, Nebraska; NC, North Carolina; ND, North Dakota; NH, New Hampshire; NJ, New Jersey; NY, New York; OH, Ohio; PA, Pennsylvania; RI, Rhode Island; SC, South Carolina; SD, South Dakota; TN, Tennessee; UT, Utah; VA, Virginia; VT, Vermont; WI, Wisconsin; WV, West Virginia; WY, Wyoming.

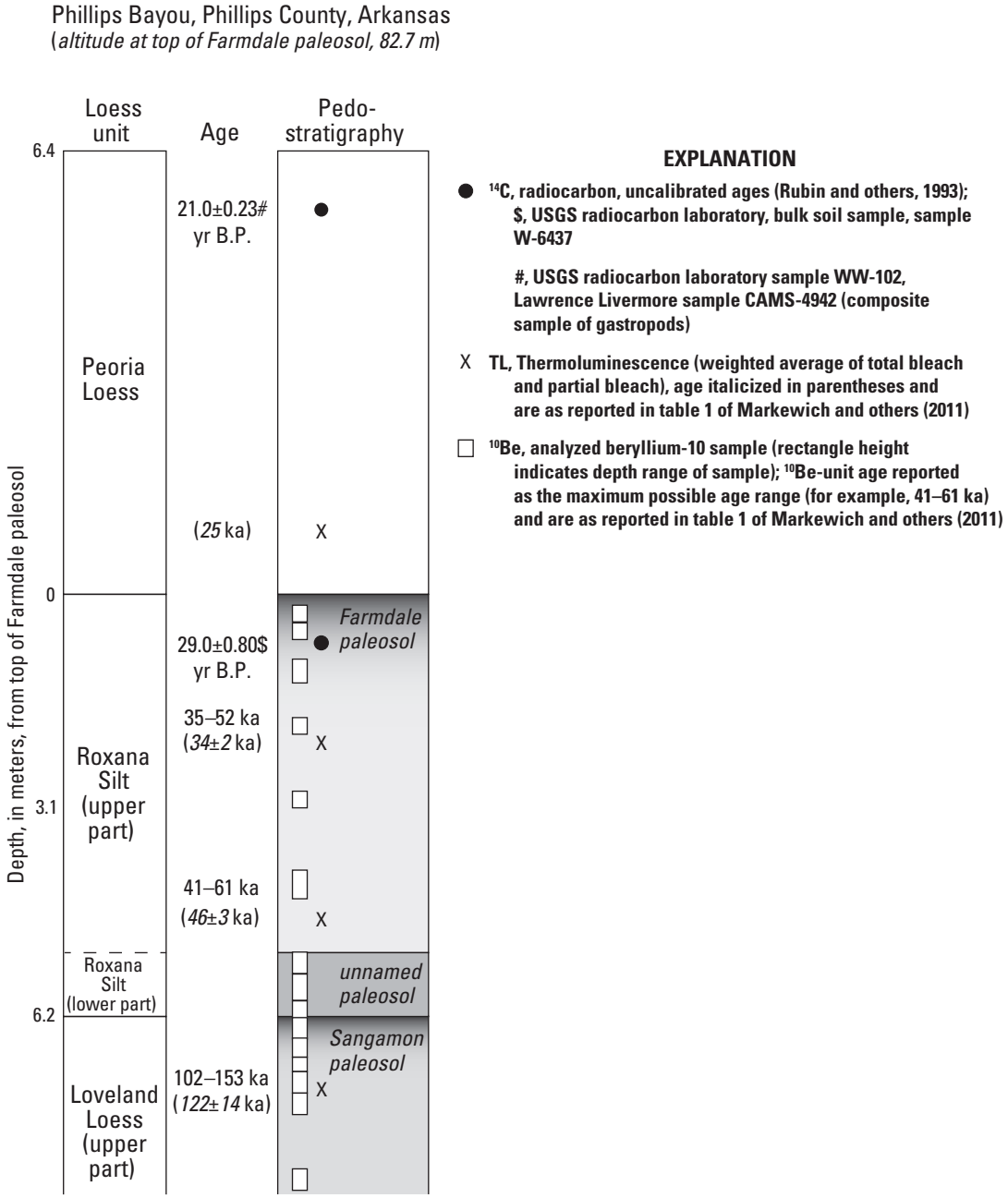

Figure 2. Stratigraphic columns showing the chronostratigraphy of the Loveland Loess, Roxana Silt, Peoria Loess, and paleosols exposed in the cut-face of an inactive quarry near the former village of Phillips Bayou, Arkansas (location shown in figure 1B). Unit names are based on previously published usage in the Mississippi Valley and for localities in western Tennessee, eastern Arkansas, and western Mississippi (Leigh and Knox, 1994; Pavich and Markewich, 1994; Leigh, 1994; Rodbell and others, 1997; Busacca and others, 2003). Unit ages and the sources for the age data are given in table 2. Figure modified from figure 2*C* in Markewich and others (2011). ka, thousand years ago; yr B.P.; years before present.

Table 1. Timeline of loess deposition, paleosol development, and interpreted paleoclimate in the lower Mississippi Valley from west-central Mississippi to east-central Missouri, southern Illinois, and southern Indiana. The marine isotope stage (MIS) age assignments are based on the LR04 stack in Railsback and others (2015); also see figure 3.

[ka, thousand years ago; MIS, marine isotope stage; ~, approximately]

Marine Isotope Stage	Time period (ka)	Loess deposition and paleosol development	Paleoclimate
Early MIS2	~30–26 ka	Peoria Loess initial deposition	Cold to very cold, windy, and dry
MIS3	~40–30 ka	Coeval Roxana Silt deposition and aggradational development of the Farmdale paleosol during a period of gradual loess deposition	Cool to cold and humid to wet
Late MIS4 through early MIS3	~50–40 ka	Gradual Roxana Silt deposition and minimal weathering	Cool to cold, windy, and subhumid to dry
Late MIS5 through MIS4	~70–50 ka	Roxana Silt deposition sufficiently slow to allow development of unnamed paleosol at contact with the Loveland Loess	Cool to cold
Late MIS5	~115–70 ka	Alternating periods of Loveland Loess deposition and Sangamon paleosol development	Cool to cold and windy alternating with warm to hot and dry
Early through middle MIS5	~130–115 ka	Sangamon paleosol development	Warm to hot and dry
MIS6	~185–130 ka	Loveland Loess deposition	Cold to very cold, windy and dry

Roxana Silt Paleosol/Loess Chronostratigraphy at Phillips Bayou

As a result of their investigations in the lower Mississippi Valley, Markewich and others (1998a, b; 2011) suggested that late MIS5 (about 115 to about 80–70 ka) Loveland Loess deposition occurred during alternating climate intervals that were cool to cold and windy, and hot and dry, with Sangamon paleosol development occurring during each of the hot and dry climate intervals. Markewich and others (1998a, b; 2010, 2011) also suggested that in the lower Mississippi Valley, MIS4–MIS3 was a transitional period of regional climate cooling, with rapid, relatively short-term (millennial to decamillennial) climatic oscillations. The overall climate was cool to cold and subhumid to humid; Roxana Silt deposition rates were low (0.10–0.25 meters [m] per 1,000 years; Pye and Johnson, 1988; Markewich and others, 1998b), and chemical weathering and pedogenesis were sufficient for development of soils with some horizonation and weakly developed structure as seen in the unnamed paleosol in the lower part of the Roxana Silt and the Farmdale paleosol in the upper part of the Roxana Silt (fig. 2). The Phillips Bayou study locality of Markewich and others (1998b, 2011) in the lower Mississippi Valley was a 30-m-high exposure on the eastern side of Crowleys Ridge, about 1 kilometer (km) south of the former village of Phillips Bayou, Arkansas (Phillips Bayou, fig. 1*B*). The exposure was about 11 km north of Helena, Arkansas, and adjacent on the west to the St. Francis River near its confluence with the Mississippi River. The St. Francis River is a small tributary of the Mississippi River that flows southward from southeastern Missouri into northeastern Arkansas along the east side of Crowleys Ridge (fig. 1*B*). The drainage basin of the St. Francis River is too small to be shown at the scale of figure 1*B*. A summary of the paleosol and loess chronostratigraphy at Phillips Bayou is in Markewich and others (1998b, 2011), and is illustrated in figure 2. The age data for the Roxana Silt at Phillips Bayou from Markewich and others (2011) are summarized in table 2. A photograph of the Phillips Bayou exposure with contacts indicated between the Loveland Loess, Roxana Silt, and Peoria Loess, as well as the paleosol/loess contacts within the Roxana Silt, is shown in figure 3. Ward and others (1993) described the complete pedostratigraphy of the Phillips Bayou thick loess section, including the about 17-m-thick Peoria Loess. The Peoria Loess was sampled by coring (Helena No. 2 core; Ward and others, 1993) upslope from the Phillips Bayou exposure because the full thickness of the Peoria Loess was not accessible from the Philips Bayou cut-face. The Phillips Bayou cut-face exposed the basal Peoria Loess, the Roxana Silt, the Loveland Loess, the Crowleys Ridge Loess, and alluvial deposits The section from the Loveland Loess through the basal Peoria Loess is shown in fig. 3. The loess section was described and sampled on vertical faces on a series of steps cut into the section. This was a necessary field decision because of the section height, slope angle, and amount of recent colluvial overburden that needed to be removed.

The Farmdale paleosol in the upper part of the Roxana Silt was tentatively considered a Cryumbrept soil by Markewich and others (1998b). The Cryumbrept great group no longer exists in “Soil Taxonomy” (Soil Survey Staff, 1975); a currently used equivalent classification is a Humicryept (Soil Survey Staff, 1999). This classification indicates a soil that has minimal horizon development and

formed when the mean annual soil temperature was higher than 0 degrees Celsius (°C) but lower than 8 °C at a 50 centimeter (cm) depth from the soil surface, and the mean winter and mean summer temperature was less than 6 °C difference at that same depth (Soil Survey Staff, 1999). Markewich and others (1998b) did not classify the unnamed paleosol in the lower part of the Roxana Silt, but noted that the unnamed paleosol had somewhat higher chroma, greater clay content, and stronger structure than the Farmdale paleosol, and possibly was welded to the underlying Sangamon paleosol.

Roxana Silt pedostratigraphy at Phillips Bayou is given in table 3 of this report and is as described by Ward and others (1993). Schoeneberger and others (1998, p. 38, Section 2, Profile/Pedon Description) defined soil structure as "the naturally occurring arrangement of soil particles into aggregates that results from pedogenic processes." Where the term "structureless" is given as the soil structure grade, the soil is either massive or single-grained. The Farmdale paleosol that developed in the Roxana Silt is massive; thus, the term "massive" has been added to the original description of Ward and others (1993).

The Roxana Silt is pedologically modified throughout. The description by Ward and others (1993) for the Roxana Silt, including the Farmdale paleosol and the unnamed paleosol, is included here (table 3) only as reference for the scanning electron microscopy/energy dispersive X-ray (SEM/EDS) analysis images. The description uses the terminology of the 1993 edition of the "Soil Survey Manual" (Soil Survey Division Staff, 1993). The terminology and field methods used by Ward and others (1993) to describe the Farmdale paleosol and the unnamed paleosol were described in Schoeneberger and others (1998). All colors in the descriptions are for moist soil or sediment (Munsell Color Company, 1992). Horizon textures were field estimates, and particle size was subsequently measured by pipette and sieve analyses by the Kellogg Soil Survey Laboratory (KSSL), Lincoln, Nebraska. In the paleosol description, the horizon texture as determined from particle size analysis is given in brackets. Measured percentages of each size fraction and other soil characterization data for the Roxana Silt were determined by the KSSL. These laboratory data are available online in the National Cooperative Soil Survey Soil Characterization Database (National Cooperative Soil Survey, undated) using lab pedon numbers 92P1024 and 92P1025. Methods of soil analyses used by the KSSL were described in the laboratory methods manual (Soil Survey Staff, 2014). Although not included in the description, the Farmdale paleosol in the upper few meters of the Roxana Silt at Phillips Bayou shows evidence of soft-sediment deformation and is bioturbated (Markewich and others, 1998b).

Table 2. Age data for the basal Peoria Loess and Roxana Silt exposed in the Phillips Bayou quarry cut-face near Phillips Bayou, Arkansas. Ages from table 1 in Markewich and others (2011).

[Site location is shown in figure 1*B*. Loess and paleosol stratigraphy shown in figure 2. ka, thousand years ago; yr B.P., year before present; cm, centimeter; ^{14}C, radiocarbon analysis; TL, thermoluminescence analysis; ^{10}Be, isotopic beryllium-10 analysis]

Dating method	Stratigraphic unit	Age	Data source and explanatory notes
^{14}C	Peoria Loess	21,070±230 yr B.P.	composite gastropod sample from 4–7 meters above the Peoria Loess/Roxana Silt contact (Rubin and others, 1993; U.S. Geological Survey Radiocarbon Laboratory sample WW-102, Lawrence Livermore sample CAMS-4942)
^{14}C	Roxana Silt, 62–85 cm depth	28,980±800 yr B.P.	bulk sample of Farmdale paleosol with charcoal flakes (Rubin and others, 1993; U.S. Geological Survey Radiocarbon Laboratory sample W-6437)
TL	Roxana Silt, upper part, 0–532 cm depth	34±2 ka	Millard and Maat (1994)
TL	Roxana Silt, lower part, 532–623 cm depth	46±3 ka	Millard and Maat (1994)
^{10}Be	Roxana Silt, upper part, 0–532 cm depth	52–35 ka	cited in Millard and Maat (1994) as personal communication from M.J. Pavich, 1993; Markewich and others (1998b)
^{10}Be	Roxana Silt, lower part, 532–623 cm depth	61–41 ka	cited in Millard and Maat (1994) as personal communication from M.J. Pavich, 1993; Markewich and others (1998b)

Figure 3. Oblique photograph of the quarry cut-face exposure near the former village of Phillips Bayou, Arkansas (lat 34.63667° N., long 90.63472° W.), showing the approximate position of contacts (dotted white lines) between the Loveland Loess and the Roxana Silt, and between the Roxana Silt and the Peoria Loess. Also shown are the Farmdale paleosol at the top of the Roxana Silt, the contact between the Farmdale paleosol and the overlying Peoria Loess, and the unnamed paleosol in the lower part of the Roxana Silt. The angle of the photograph is an upward oblique view from a point near the lower part of the Loveland Loess. This view gives a skewed perspective of the Roxana Silt thickness. The Farmdale paleosol in the image is on higher step, which is not completely visible. The Roxana Silt is 6.23 meters (m) thick. The image shows the upper 1.5 to 2.0 m of the 3.25-m thick Sangamon paleosol that formed in the 7.3-m thick Loveland Loess. The contact between the Sangamon paleosol and the overlying unnamed paleosol is the contact between the Loveland Loess and the overlying Roxana Silt. D.A. Wysocki is in the photograph. Photograph taken by H.W. Markewich, U.S. Geological Survey.

Table 3. Paleosol/loess stratigraphy for the Roxana Silt section of the Phillips Bayou exposure as described by Ward and others (1993).

[Site location is shown in figure 1. Location used by Ward and others (1993) for both the described cut-face and the Helena No. 2 core: lat 34.63667° N., long 90.63472° W., Phillips County, Arkansas. Horizon texture as determined from particle size analysis is given in brackets. Field pedon number of Ward and others (1993): 92PH02; lab pedon numbers: 92P1024 and 92P1025; depth measurements taken down from datum at 85.5 meters elevation, top of Farmdale paleosol. ka, one thousand years before present; cm, centimeter; %, percent; <, less than; mm, millimeters; Fe, iron; Mn, manganese ^{14}C, radiocarbon analysis]

Paleosol name	Horizon designation	Horizon depths, in cm	Horizon description
Farmdale paleosol	2A1	0–17	Dark brown (10*YR* 4/3) silt loam [silt loam]; common medium distinct gray (l0*YR* 5/1) and common medium distinct strong brown (7.5*YR* 4/6) mottles; structureless, massive; friable; few very fine, few fine, and occasional medium pores; about 50% of pores have oxidized walls; few (<1%) fine and medium (2–4 mm) hard round black to brown Fe and Mn concretions; clear smooth boundary. Few krotovinas known from this horizon, but not in the described section (fig. 3).
	2A2	17–43	Dark grayish brown (l0*YR* 4/2) silt loam [silt loam]; common medium distinct dark yellowish brown (l0*YR* 4/3) and common fine and medium faint dark brown (10*YR* 3/2) mottles; structureless, massive; friable; few very fine and few fine pores; about 30% of pores have oxidized walls; two horizontal dark yellowish brown (10*YR* 4/6) oxidation bands about 5 mm wide occur near base of horizon; few (<1%) fine and medium (2–4 mm) hard round gray calcium carbonate concretions; few (<1%) fine and medium (2–4 mm) hard round black to brown Fe and Mn concretions; clear smooth boundary.
	2A3	43–62	Dark grayish brown (10*YR* 4/2) silt loam [silt loam]; many fine and medium faint dark brown (10*YR* 3/2) mottles; structureless, massive; friable; few very fine and fine pores; few (<1%) fine (1–2 mm) hard round black-brown Fe and Mn concretions; gradual smooth boundary.
	2A4	62–85	Dark brown (10*YR* 3/2) silt loam [silt loam]; few fine distinct strong brown (7.5*YR* 4/6) mottles; structureless, massive; friable; few very fine and fine pores; many pale brown (10*YR* 6/3) uncoated silt grains on fracture faces; few irregular shaped pockets of pale brown (10*YR* 6/3) uncoated silt grains 5–10 mm in diameter; clear smooth boundary. ^{14}C age determination for disseminated organics in this horizon is 28,980±800 yr B.P. (table 2 in this report).
	2A5	85–96	Dark brown (10*YR* 3/2) silt loam [silt loam]; structureless, massive; friable; few very fine and fine pores; many pale brown (10*YR* 6/3) uncoated silt grains on fracture faces; common irregular shaped pockets of pale brown (10*YR* 6/3) uncoated silt grains 2–10 mm in diameter; few (<1%) fine and medium (2–4 mm) brown hard round Fe and Mn concretions; clear smooth boundary.
	2Bt1	96–184	Brown (10*YR* 5/3) silt loam [silt loam]; common medium distinct yellowish brown (10*YR* 5/6) mottles; structureless, massive (possibly very weak to weak coarse sub-angular blocky); friable; many very fine, many fine and few medium pores; most fine and medium pores lined with yellowish red (5*YR* 4/6) clay; most of remaining pores have strong brown (7.5*YR* 4/6) oxidized pore walls; 2 krotovinas 6–8 cm in diameter filled with dark grayish brown (10*YR* 4/2) silt loam; 6–8 horizontal to diagonal strong brown (7.5*YR* 5/6, 5/8) oxidation bands across horizon on shaved face, appear to be common medium distinct yellowish brown (10*YR* 5/6) mottles on picked face; common (2%) fine (1–2 mm) hard round black to brown Fe and Mn concretions; gradual smooth boundary. Subsampled: 96–140 cm depth; 140–184 cm depth.
	2Bt2	184–285	Pale brown (10*YR* 6/3) silt loam [silt loam]; few medium distinct yellowish brown (10*YR* 5/6) mottles; structureless; friable; many very fine, many fine and many medium pores; most fine and medium pores lined with yellowish red (5*YR* 4/6) clay; most of remaining pores have strong brown (7.5*YR* 4/6) oxidized pore walls; few (1%) fine (1–2 mm) hard round black to brown Fe and Mn concretions; clear smooth boundary. Subsampled: 184–218 cm depth; 218–252 cm depth; 252–285 cm depth.

Table 3. Paleosol/loess stratigraphy for the Roxana Silt section of the Phillips Bayou exposure as described by Ward and others (1993).—Continued

[Site location is shown in figure 1. Location used by Ward and others (1993) for both the described cut-face and the Helena No. 2 core: lat 34.63667° N., long 90.63472° W., Phillips County, Arkansas. Horizon texture as determined from particle size analysis is given in brackets. Field pedon number of Ward and others (1993): 92PH02; lab pedon numbers: 92P1024 and 92P1025; depth measurements taken down from datum at 85.5 meters elevation, top of Farmdale paleosol. ka, one thousand years before present; cm, centimeter; %, percent; <, less than; mm, millimeters; Fe, iron; Mn, manganese ^{14}C, radiocarbon analysis]

Paleosol name	Horizon designation	Horizon depths, in cm	Horizon description
Farmdale paleosol —Continued	2Bt3	285–359	Light yellowish brown (10*YR* 6/4) silt loam [silt]; few medium distinct yellowish brown (10*YR* 5/6) mottles; structureless, massive; friable; many very fine, many fine and many medium pores; most fine and medium pores lined with yellowish red (5*YR* 4/6) clay; most of remaining pores have strong brown (7.5*YR* 4/6) oxidized pore walls; few horizontal and vertical yellowish brown (10*YR* 5/6) oxidation bands 5–10 mm wide across horizon; few (1%) fine (1–2 mm) hard round black to brown Fe and Mn concretions; gradual smooth boundary. Subsampled: 285–322 cm depth; 322–359 cm depth.
	2Bt4	359–415	Light yellowish brown (10*YR* 6/4) silt [silt loam]; few medium distinct brownish yellow (10*YR* 6/6) mottles; structureless, massive; friable; common very fine, common fine and common medium pores; most fine and medium pores lined with yellowish red (5*YR* 4/6) clay; most of remaining pores have strong brown (7.5*YR* 4/6) oxidized pore walls; 3 diagonal yellowish brown (10Y*R* 5/6) oxidation bands 1–2 cm wide across horizon; common (2%) fine (1–2 mm) hard round black-to brown Fe and Mn concretions; diffuse smooth boundary. Subsampled: 359–387 cm depth; 387–415 cm depth.
	2Bt5	415–532	Strong brown (7.5*YR* 5/4) silt [silt loam]; structureless, massive; friable; common very fine, common fine and common medium pores; most fine and medium pores lined with yellowish red (5*YR* 4/6) clay; most of remaining pores have strong brown (7.5*YR* 4/6) oxidized pore walls; few distinct pockets of pale brown (10*YR* 6/3) uncoated silt grains 2-10 mm in diameter; common (2%) fine (1–2 mm) hard round black-brown Fe and Mn concretions; diffuse smooth boundary. Subsampled: 415–454 cm depth; 454–493 cm depth; 493–532 cm depth.
Unnamed paleosol	2At	532–594	Brown (10*YR* 4/3) silt loam [silt loam]; common medium distinct strong brown (7.5*YR* 4/6, 5/6) mottles; weak medium and coarse angular blocky structure; friable; many very fine, common fine and common medium pores; many fine and medium pores lined with yellowish red (5*YR* 4/6) clay; most very fine pores have strong brown (7.5*YR* 4/6) oxidized pore walls; few distinct pale brown (10*YR* 6/3) and very pale brown (10*YR* 7/3) uncoated silt grains on faces of peds; common (2%) fine (1–2 mm) hard round black-to brown Fe and Mn concretions; gradual smooth boundary. Appears to be welded to the Sangamon paleosol at top of Loveland Silt (Loess). Subsampled: 532–568 cm depth; 568–594 cm depth.
	2ABt	594–623	Dark yellowish brown (l0*YR* 4/4) silt loam [silt loam]; common fine and medium distinct strong brown (7.5*YR* 4/6, 5/6) mottles; weak medium and coarse angular blocky structure; friable; many very fine, many fine and common medium pores; many fine and medium pores lined with yellowish red (5*YR* 4/6) clay; most very fine pores have strong brown (7.5YR 4/6) oxidized pore walls; common distinct pale brown (10*YR* 6/3) and very pale brown (10*YR* 7/3) uncoated silt grains on faces of peds; common (2%) fine and medium (l–5 mm) hard round black to brown Fe and Mn concretions; gradual wavy boundary.

SEM/EDS Investigations of the Roxana Silt at Phillips Bayou

At the Phillips Bayou exposure, samples of the Roxana Silt were taken for SEM/EDS analysis in 1992 (Ward and others, 1993) and 1994. Samples for SEM/EDS analysis of the Roxana Silt exposed in the Phillips Bayou quarry cut-face were taken originally from May 29 through June 5, 1992, by D.A. Wysocki. Markewich and others (1998a, b) discussed the initial results of this SEM/EDS investigation. The objectives of the SEM/EDS study were to consider the depositional environment, the post-depositional weathering intensity, and identify any discontinuities in the deposition of the Roxana Silt. Specifically, the SEM/EDS study was to identify changes in grain characteristics and morphology within the Roxana Silt for paleoenvironmental interpretation (Markewich and others, 1998a, b). Although the results were summarized in articles by Markewich and others (1998a, b, 2010), the mineralogical and morphological data from the SEM/EDS analysis were not published.

On June 22, 1994, J.B. Dixon and D.A. Wysocki took additional samples at the Phillips Bayou exposure to supplement the original sample set taken in 1992. All loess samples were examined and analyzed by G.N. White and J.B. Dixon in the facilities of the Soil and Crop Sciences Department, Texas A&M University, College Station, Texas. Observations and several images from their SEM/EDS analysis are presented in the Materials and Methods and the Results of SEM/EDS Analysis sections of this report. Depths for analyzed samples are the same as the horizon depths in the pedostratigraphic description of Ward and others (1993) (table 3). Soil horizon depths were measured from the top of the Farmdale paleosol at its contact with the overlying Peoria Loess. Horizon nomenclature and depths for samples of Roxana Silt examined for the SEM/EDS study are 2A1 (0–17 cm), 2Bt1 (96–140 cm), 2Bt2 (218–252 cm), 2Bt4 (359–387 cm), and 2ABt (594–623 cm). Samples from 0–387 cm depth are from the Farmdale paleosol that developed in the upper part of the Roxana Silt. The sample from 594–623 cm depth is from the unnamed paleosol that developed in the basal Roxana Silt. For discussion purposes, samples from 0 to 359 cm depth (2A1, 0–17 cm; 2Bt1, 96–140 cm; 2Bt2, 218–252 cm) are considered to be from the upper part of the Roxana Silt, and samples from 359 cm to 623 cm depth (2Bt4, 359–387 cm; 2ABt, 594–623 cm) are considered to be from the lower part of the Roxana Silt (fig. 2).

Materials and Methods

Samples were separated into sand (wet sieving), silt, and clay (centrifugation and sedimentation) fractions for further examination using a dilute sodium carbonate (Na_2CO_3) solution as a dispersant with no other pretreatments (Dixon and White, 1993, 1999). Carbonate minerals were not removed to allow examination of the surface textures of individual dolomite or calcite grains, if present. KSSL data show that the Roxana Silt 2A1 (0–17 cm) horizon has a calcium carbonate ($CaCO_3$) equivalent of 2 percent in the less than 2-millimeter (mm) size fraction, and that upon conducting the KSSL hydrochloric acid response test, reaction with hydrochloric acid responded slowly. These data indicate that the Roxana 2A1 horizon was enriched with dolomite by reworking from the overlying Peoria Loess. Optical grain counts for 300 grains conducted by the KSSL show abundant calcite in the Peoria Loess from 30 cm (11 percent calcite) and 160 cm (22 percent calcite) above the Roxana Silt contact. No grain count was conducted on the Roxana Silt 2A1 (0–17 cm) horizon. A grain count on the Roxana Silt 2A2 (17–43 cm) showed no calcite. Distinguishing dolomite from calcite is difficult in optical grain counts, so the KSSL grain counts include dolomite with calcite. Neither calcite nor dolomite was identified in the grain counts conducted for SEM/EDS analysis, which used the grain morphology and the energy dispersive X-ray (EDS) patterns.

Sand and silt grains were secured to a 10-mm diameter aluminum stub with carbon adhesive, coated with 100×10^{-10} meter-sized gold (Au) particles to reduce charging, and examined using a JEOL 6400 scanning electron microscope (SEM) with a Tracor Northern EDS analysis unit. Samples were placed into the SEM and then examined with an operating voltage of 25 kiloelectron volts. Minerals were identified by using the grain morphology and the EDS patterns (table 4; Dixon and White, 1993,1999; White, 2008). Elements with an atomic number of 11 (sodium) or greater were assumed detectable by EDS. The morphology of sand- and silt-sized quartz and weatherable minerals was examined closely because these minerals aid in determining depositional environment and evaluating the post-depositional weathering regime. Grain counts were performed on samples to reduce bias in choosing representative grains for photography. In the sand size fraction, the number of counted grains ranged from 121 to 20. In the silt fraction, the number of counted grains ranged from 167 to 91. Many grains were heavily coated with iron (Fe) oxides, especially in the sand size fraction (fig. 4). These iron-oxide coatings hindered examination of grain morphology and mineral identification, which resulted in a low number of counted grains in the sand size fraction. The sand fraction for sample 2Bt1 (96–140 cm depth) had a total grain count of only 20.

Table 4. Recognition criteria used for mineral identification for soil minerals observed by scanning electron microscopy/energy dispersive X-ray spectroscopy (SEM/EDS) analysis. Minerals are arranged in the approximate order of decreasing frequency of occurrence in developed soils. Other minerals may occur in soils, but their morphology and chemistry are not distinctive enough for use in mineral identification without corroborating X-ray diffraction data. Table is from Dixon and White (1993, table 1–2, p. 12–13).

[EDS, energy dispersive X-ray spectroscopy; Si, silicon; Al, aluminum; K, potassium; Mg, magnesium; Fe, iron; Na, sodium; Ca, calcium; Mn, manganese; Ti, titanium; Zr, zircon; S, sulfur; —, not applicable]

Mineral	Variety	Criteria for identification
Quartz	—	Si-only EDS spectra and morphology
Muscovite	—	Al peak almost equal in height to the Si peak, K peak about 0.3 as intense, and platy morphology
Biotite	—	Si peak about 3 times K peak with Al, Mg, and Fe EDS peaks as intense as the Si peak; No Na or Ca peaks
Kaolinite	—	Al peak almost equal in height to Si peak, and no significant Na, Ca, or K; platy morphology
Smectite	—	Very thin platy morphology with minor Na or Ca depending upon cation saturation, and stronger Mg, Al, Si, and Fe peaks, and little or no K in EDS (assuming cation saturation is known); usually too small for observation as single crystals but observed as a matrix
Vermiculite	—	Thicker platy morphology than smectite, with stronger Na or Ca EDS peaks depending upon cation saturation, and significant Mg, Al, Si, and Fe peaks, and little or no K in EDS (assuming cation saturation is fixed)
Illite	—	Thin-to-thick platy morphology with Na or Ca in small concentrations, Mg, Al, Si, and Fe peaks, and K equal or less than that of muscovite or biotite
Halloysite	—	Al peak almost equal in height to Si peak, tubular morphology, and no significant Na, Ca, or K.
Chlorite	—	Platy morphology with varying amounts of Fe, Mg, Mn, Al, and Si in EDS pattern with negligible Na, Ca, or K.
Feldspar	—	Strong Al and Si EDS peaks with Na, K, or Ca EDS peaks only; often exhibits good cleavage in 2 directions at or close to 90°, and preferential weathering based on cationic substitution.
	Microcline	K and Al EDS peaks about 0.3 as intense as Si
	Orthoclase	Same composition as microcline, indistinguishable from microcline by EDS
	Sanidine	Like orthoclase with some Na substitution
	Sodic plagioclase	Na peak greater than half Al peak, which is about a third as intense as Si in EDS; may have some Ca replacing the Na
	Calcic plagioclase	Ca peak about half the height of the Al peak, which is nearly as intense as the Si EDS peak
Fe oxides	—	Very hard to distinguish by SEM except in unusual cases where the morphology is distinctive and evident; all show Fe EDS peak only
	Hematite	Rarely has observable platy morphology
	Lepidocrocite	Rarely has observable platy morphology
	Ferrihydrite	Granular morphology almost too small for observation in SEM even as a matrix
	Goethite	Prismatic or acicular crystals sometimes large enough for observation with SEM
Carbonates	—	Sometimes have rhombohedral morphology
	Calcite	Ca EDS peak only, may be hard to distinguish from gypsum by EDS alone
	Dolomite	Ca peak nearly twice height of Mg peak in EDS
	Siderite	Fe peak alone or with minor Ca
Ilmenite	—	Fe and Ti only in EDS spectra, nearly same peak height
Zircon	—	Zr and Si EDS peaks
Rutile	—	Ti peak only in EDS and prismatic morphology
Anatase	—	Ti peak only in EDS and non-prismatic morphology

Table 4. Recognition criteria used for mineral identification for soil minerals observed by scanning electron microscopy/energy dispersive X-ray spectroscopy (SEM/EDS) analysis. Minerals are arranged in the approximate order of decreasing frequency of occurrence in developed soils. Other minerals may occur in soils, but their morphology and chemistry are not distinctive enough for use in mineral identification without corroborating X-ray diffraction data. Table is from Dixon and White (1993, table 1-2, p. 12–13).—Continued

[EDS, energy dispersive X-ray spectroscopy; Si, silicon; Al, aluminum; K, potassium; Mg, magnesium; Fe, iron; Na, sodium; Ca, calcium; Mn, manganese; Ti, titanium; Zr, zircon; S, sulfur; —, not applicable]

Mineral	Variety	Criteria for identification
Gibbsite	—	Ai EDS peak only and platy morphology
Gypsum	—	Ca and S EDS peaks nearly equal in intensity (Note: S EDS peak overlaps with Au coating peak and may not be observable for this and other sulfur-containing minerals)
Barite	—	Ba and S EDS peaks only
Pyrite	—	Fe and S EDS peaks, usually with octahedral or cubic crystal faces
Marcasite	—	Fe and S EDS peaks, with rounded crystal faces and no octahedral or cubic faces
Halite	—	Na and Cl EDS peaks, often with a cubic morphology
Sphene	—	Ca, Ti, and Si in EDS pattern

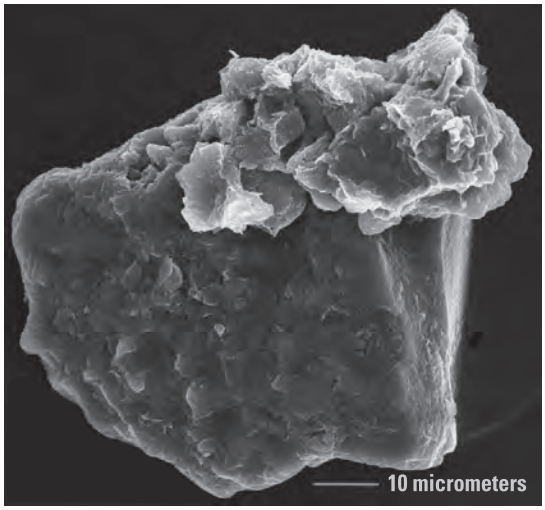

Figure 4. Scanning electron microscope photograph of an iron oxide-coated sand-sized quartz grain from 594–623 centimeters depth (2ABt soil horizon, unnamed paleosol in the lower part of the Roxana Silt [figs. 2, 3; table 3]), with a silt-sized iron oxide-coated potassium feldspar or muscovite grain on the quartz grain. Photograph by G.N. White.

Results of SEM/EDS Analysis

Grain counts and mineral identification performed on the samples during SEM/EDS examination showed the samples to be composed dominantly of quartz and feldspars with minor amounts of weatherable minerals (for example, pyroxene and amphibole), mica, and resistant heavy minerals (for example, rutile and sphene). The amounts of feldspars and quartz present in the samples are consistent across the sand and silt fractions, but the content of weatherable minerals, mica, and resistant heavy minerals is variable but somewhat higher in the silt fraction.

In both the sand and silt fractions, the upper part of the Roxana (0–359 cm depth, fig. 2) contains less quartz and more feldspar compared to the lower part of the Roxana (359–623 cm depth, fig. 2). Excluding the sample from the 2Bt1 (96–140 cm depth) because of the low total grain count, the sand fraction in the upper part has weighted average quartz and feldspar percentages of 65 percent and 34 percent, respectively. The sand fraction in the lower part has weighted average quartz and feldspar percentages of 76 percent and 21 percent, respectively. The silt fraction in the upper part has weighted average quartz and feldspar percentages of 54 percent and 34 percent, respectively. The silt fraction in the lower part has weighted average quartz and feldspar percentages of 72 percent and 25 percent, respectively. The higher quartz and lower feldspar values in the lower part possibly are due to incorporation of weathered quartz-rich material from the underlying Sangamon paleosol that developed in the Loveland Loess (fig. 2).

In the sand and silt size fractions in all samples, the potassium feldspar percentage was greater than the percentage of plagioclase. The percentage of intermediate plagioclase was greater than the combined percentage of calcium plagioclase and sodium plagioclase. The percentage of weatherable minerals, mica, and resistant heavy minerals ranged from 5 percent to 0 in the sand size fraction and from 9 percent to 0 in the silt size fractions. Other minerals occur in the Roxana Silt paleosols, but their morphology and chemistry are not distinctive enough for mineral identification without corroborating X-ray diffraction data.

Examination of the quartz sand surface features using the system of Krinsley and Doornkamp (1973) showed many of the grains to have cleavage faces and striated conchoidal fractures (fig. 5), although many grains were coated with iron oxides, making detailed examination of surface morphology impossible (fig. 4). Rare, rounded quartz sand grains were also observed (fig. 6*A*), and a close-up of the surface of the grain in figure 6*B* shows an unusual texture of deep, elongated pits separated by irregular ridges. The pits appear to be following a crystallographic direction from left to right in figure 6*B*, possibly the result of dissolution along structure or stress features. This kind of pitted, ridged texture was not recorded by Krinsley and Doornkamp (1973).

Quartz morphology in the silt was similar to that observed in the sand, with sharp edges, prominent striated conchoidal fractures, and cleavage features (fig. 7*A*, *B*) that suggest a glacial origin (Mahaney, 2002). Primary surface features resulting from deposition processes may have been hidden on many grains by silica overgrowths (fig. 8*A*, *B*) or by quartz crystal faces (fig. 8*C*, *D*) that resulted from extensive quartz overgrowths.

Feldspar grains in the Roxana Silt generally showed more signs of weathering than did quartz grains. Although most potassium feldspar grains, especially those of sand size, showed only minor weathering (fig. 9*A*), some silt-size potassium feldspar grains showed surface pitting (fig. 9*B*). Intermediate plagioclase grains (fig. 9*C*, *D*) were more weathered than the potassium feldspar and somewhat more weathered than end-member (anorthite, $CaAl_2Si_2O_8$) plagioclase grains. In some cases, etching of the plagioclase grains appeared to be crystallographically controlled (fig. 9*C*).

Other minerals also were observed in the samples from the Philips Bayou section, especially in the silt fractions. Pyroxenes and amphiboles were common constituents of the silt fractions of the entire section. Most grains appeared relatively unweathered (fig. 10*A*), but some were partially or highly weathered (fig. 10*B*). Titanium oxides appeared as rutile (fig. 11*A*), which probably is a primary mineral, as well as in secondary mineral forms (fig. 11*B*). Other mineral forms of titanium included sphene (fig. 11*C*) and ilmenite (fig. 11*D*). Muscovite also was observed, and most grains appeared to exhibit the initial stages of delamination due to potassium loss (fig. 12).

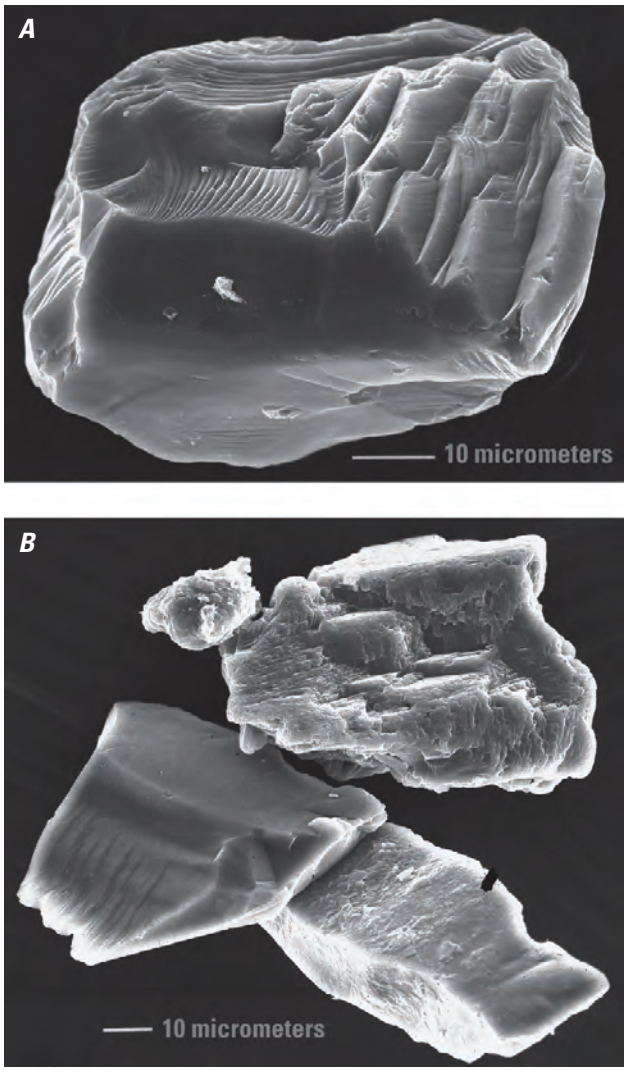

Figure 5. Scanning electron microscope photographs of quartz sand grains and a potassium feldspar sand grain from 594–623 centimeters depth, 2ABt soil horizon, unnamed paleosol in the lower part of the Roxana Silt (figs. 2, 3; table 3). *A*, Quartz grain with cleavage faces and conchoidal fracturing striated by subparallel linear fractures that are indicative of glacial crushing processes (Immonen, 2013; Woronko and Pisarska-Jamroży, 2016). *B*, Quartz and potassium feldspar grains. The upper grain is potassium feldspar showing cleavage faces and some surface weathering. The center left grain is quartz with striated conchoidal fractures. The lower right grain is also quartz with a very thin coating of amorphous silica. Photograph by G.N. White.

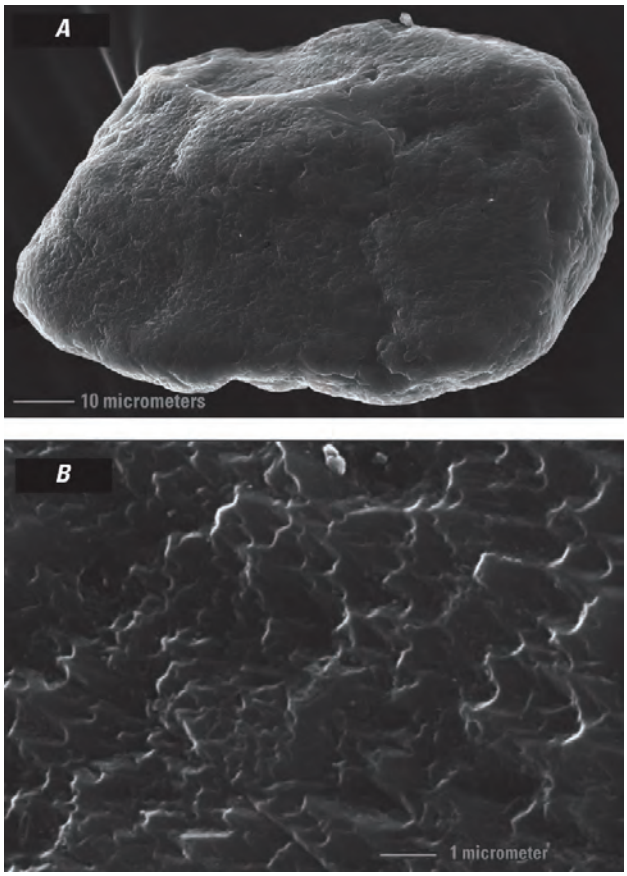

Figure 6. Scanning electron microscope photograph of a rounded quartz sand grain from 594–623 centimeters depth, 2ABt soil horizon, unnamed paleosol in the lower part of the Roxana Silt (figs. 2, 3; table 3). *A*, Whole grain. *B*, Close-up of grain surface showing unusual surface texture/topography. Photograph by G.N. White.

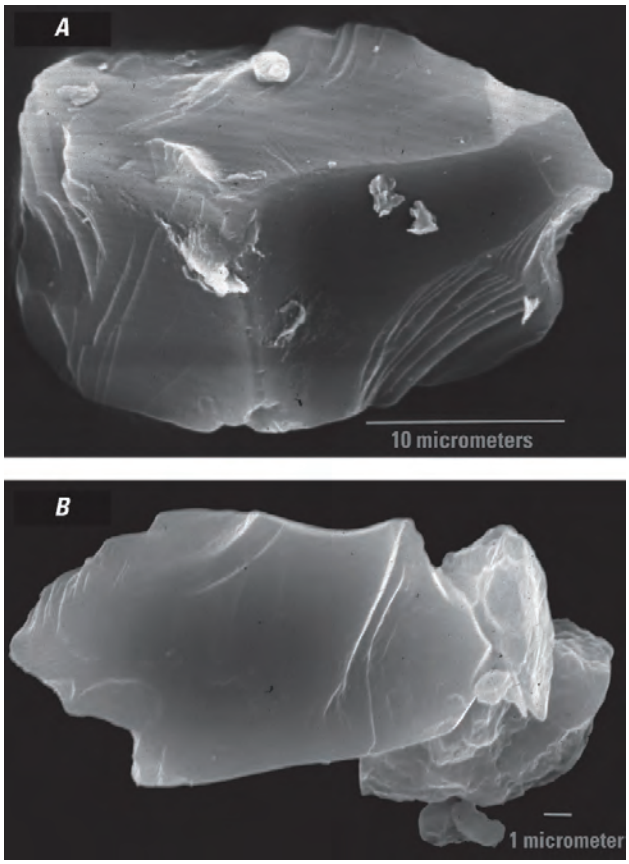

Figure 7. Scanning electron microscope photographs showing quartz silt grain morphologies. *A*, Quartz silt grain from 96–140 centimeters (cm) depth, 2Bt1 soil horizon, Farmdale paleosol (figs. 2, 3; table 3) with sharp grain edges, prominent striated conchoidal fractures, and cleavage features. *B*, Quartz silt grain (largest grain in the foreground) from 0–17 cm depth, 2A1 soil horizon, Farmdale paleosol (figs. 2, 3; table 3), with extensive conchoidal fracturing. Photograph by G.N. White.

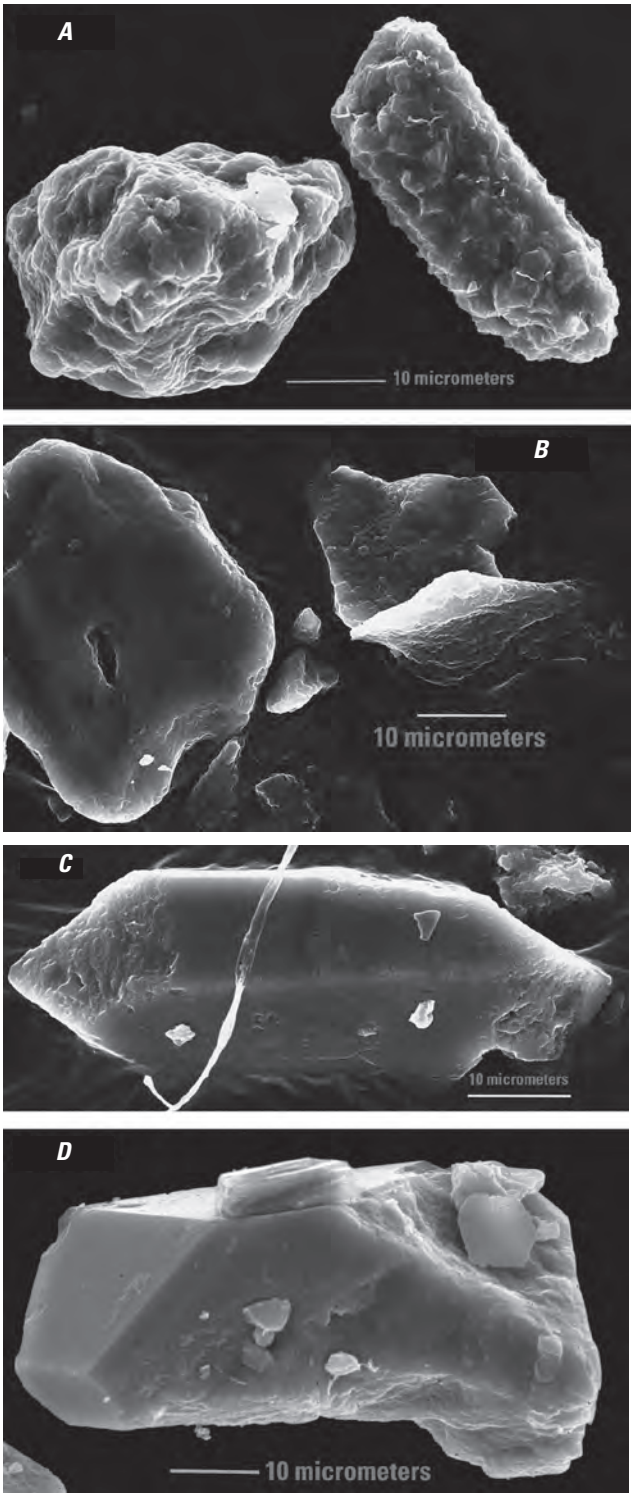

Figure 8. Scanning electron microscope photographs of quartz silt grains with no visible depositional features (no abrasion features caused by the agent of deposition, such as wind [eolian] or water [fluvial]). *A*, Two quartz silt grains from 96–140 centimeters (cm) depth, 2Bt1 soil horizon, Farmdale paleosol (figs. 2, 3; table 3) with depositional features covered by silica overgrowths. *B*, Three quartz silt grains with extensive overgrowths, also from 96–140 cm depth. Note the hole in the overgrowth on the grain on the left. *C*, Quartz silt grain from 218–252 cm depth, 2Bt2 soil horizon, Farmdale paleosol (figs. 2, 3; table 3) showing quartz hexagonal prism faces resulting from secondary quartz precipitation. *D*, Quartz silt grain from 96–140 cm depth, 2Bt1 soil horizon, Farmdale paleosol (figs. 2, 3; table 3) showing rhombohedral and hexagonal prism crystal faces as the result of extensive quartz overgrowth. Photograph by G.N. White.

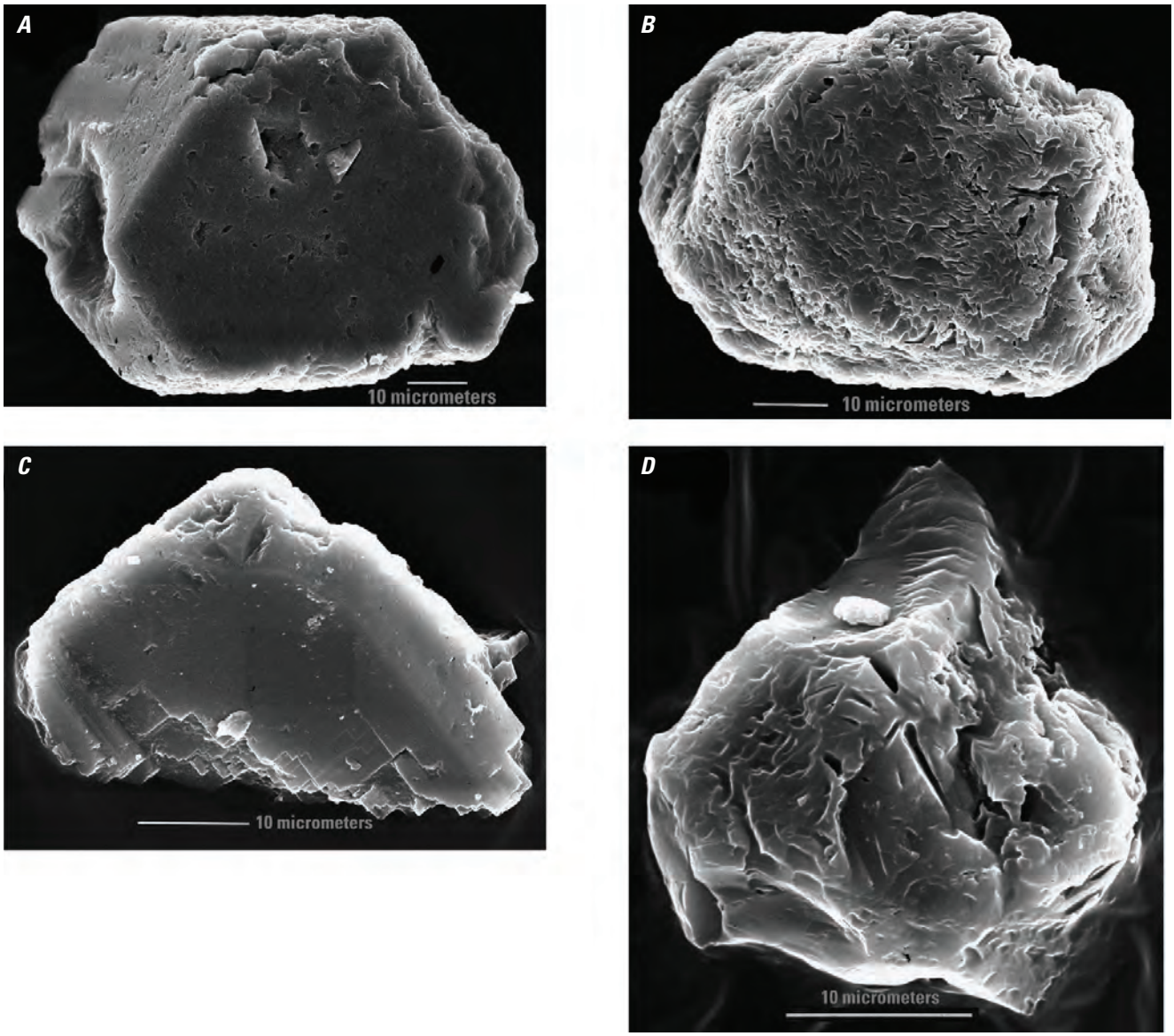

Figure 9. Scanning electron microscope photographs of feldspar grain morphologies. *A*, Potassium feldspar very fine sand grain from 96–140 centimeters (cm) depth, 2Bt1 soil horizon, Farmdale paleosol (figs. 2, 3; table 3) with relatively limited weathering represented by intact cleavage and crystal growth faces. *B*, Potassium feldspar coarse silt grain from 594–623 cm depth, 2ABt soil horizon, unnamed paleosol in the lower part of the Roxana Silt (figs. 2, 3; table 3) that displays moderate weathering represented by pitted grain surfaces and worn-down cleavage and crystal faces. *C*, Intermediate plagioclase silt grain from 218–252 cm depth, 2Bt2 soil horizon, Farmdale paleosol (figs. 2, 3; table 3), with grain surfaces altered along crystallographic directions. *D*, Intermediate plagioclase silt grain that is rounded with weathered surfaces, also from 218–252 cm depth. Photograph by G.N. White.

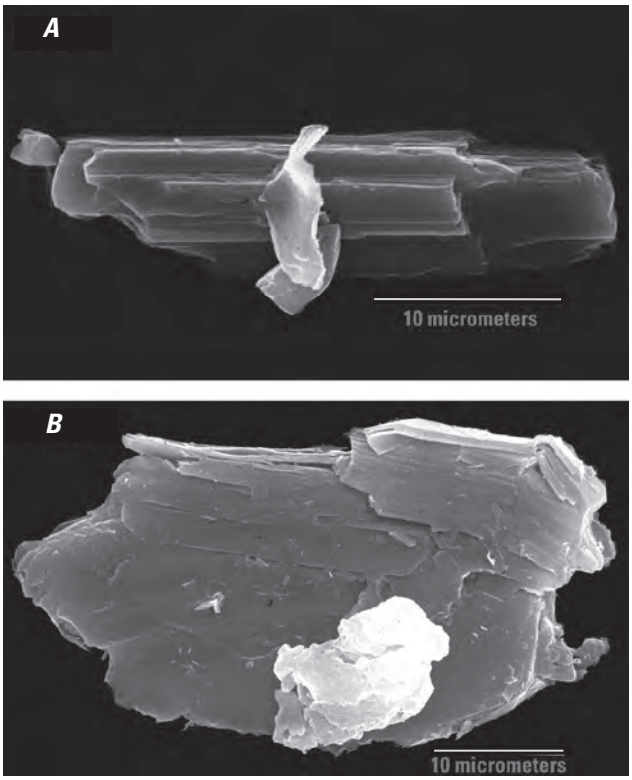

Figure 10. Scanning electron microscope photographs of surface morphologies of pyroxenes and amphiboles or both. *A*. Unweathered silt grain from 0–17 centimeters (cm) depth, 2A1 soil horizon, Farmdale paleosol (figs. 2, 3; table 3) with characteristic inosilicate elongate morphology. *B*, An inosilicate silt grain (amphibole or pyroxene), also from 0–17 cm depth, showing crystallographically controlled weathering features. Photograph by G.N. White.

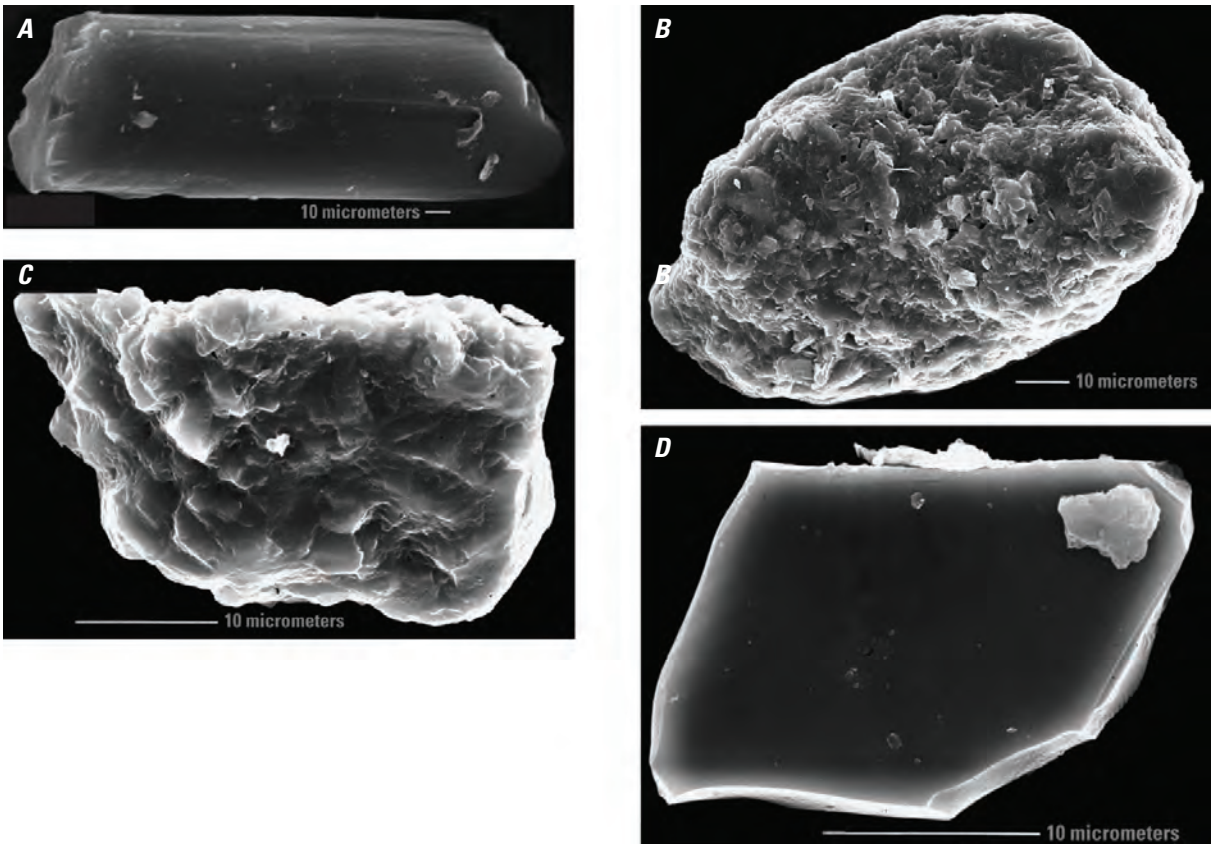

Figure 11. Scanning electron microscope photographs of titanium oxide morphologies. *A*, Rutile sand grain from 594–623 centimeters (cm) depth, 2ABt soil horizon, unnamed paleosol in the lower part of the Roxana Silt (figs. 2, 3, table 3) *B*, Unknown titanium-oxide aggregate sand grain from 359–387 cm depth, 2Bt4 soil horizon, Farmdale paleosol (figs. 2, 3; table 3). *C*, Sphene silt grain from 96–140 cm depth, 2Bt1 soil horizon, Farmdale paleosol (figs. 2, 3; table 3). *D*, Ilmenite silt grain also from 96–140 cm depth. Photograph by G.N. White.

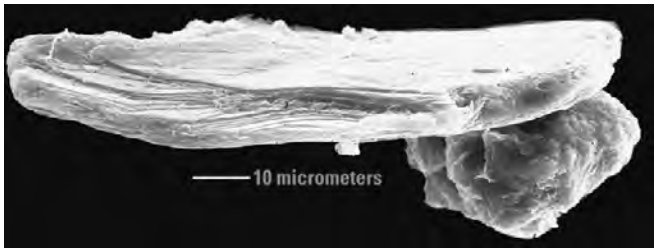

Figure 12. Scanning electron microscope photograph of a muscovite sand grain from 359–387 centimeters depth, 2Bt4 soil horizon, Farmdale paleosol (figs. 2, 3; table 3) showing some delamination from weathering. Below the muscovite sand grain is a silt grain of pitted feldspar. Photograph by G.N. White.

Summary of SEM/EDS analysis

The primary morphology of quartz sand grains from the Roxana Silt is irregularly shaped grains with sharp, conchoidal fracturing, striations, and an angular outline. This type of morphology occurs with high frequency in glacial environments because of grain-to-grain contact and high shear stress found in these kinds of environments (Mahaney, 2002; Woronko and Pisarska-Jamroży, 2016). There are few well-rounded sand grains, which are formed as a result of repeated saltation either in water or during eolian processes. The lack of rounded grains in the Roxana Silt suggests that most grains did not undergo multiple cycles of transport and deposition prior to loess transport. The limited grain-rounding reflects the initial glacial origin (pressure fracturing and shearing) and relatively rapid deposition via meltwater throughout the Mississippi Valley during deglaciation.

There were no major differences in the feldspars and other minerals as a function of depth in the Roxana Silt, which suggests that this loess was derived from a consistent source. The lack of large differences in weathering intensity with depth suggests a relatively consistent rate of sediment addition with no long periods of surface weathering. There also is a minimal degree of weathering near the top of the Roxana Silt in the Farmdale paleosol. One explanation for this lack of weathering differences might be that the mixing of new material by pedoturbation reduced the degree of weathering differences with depth. Alternatively, the weathered upper portion of the Roxana Silt may have been eroded prior to

Peoria Loess deposition. Feldspar grains (fig. 9) in the Roxana Silt display slightly more surface weathering than quartz (figs. 7, 8), and this feldspar weathering would yield some clay, but in an insufficient amount for noticeable argillans or plasma development, which is consistent with the limited chemical weathering associated with Farmdale paleosol pedogenesis that has been documented in northeastern Illinois (Jacobs and others, 2009). Abundant dolomite in the 2A1 horizon of the Farmdale paleosol possibly is the result of pedoturbation during deposition of the overlying Peoria Loess, which contains abundant dolomite.

Observations

- Results of the SEM/EDS analysis of the Roxana Silt at Phillips Bayou presented in this report do not directly address the question of the presence or absence of the Laurentide Ice Sheet in the upper Mississippi Valley at the time of Roxana Silt deposition. The morphological data from grains analyzed by SEM/EDS and previously published pedologic data (table 3; Markewich and others, 1998b) support published paleoclimatic interpretations for MIS5–MIS3 loess deposition in the unglaciated lower Mississippi Valley as far south as west-central Mississippi (Markewich and others, 1998a, b, 2011). The data indicate a cool to cold and humid climate with coincident slow rates of loess deposition, mineral weathering, and pedogenesis during MIS4–MIS3. The unnamed paleosol in the lower part of the Roxana Silt appears to be somewhat more developed than the Farmdale paleosol, and if this is the case, then the unnamed paleosol possibly is evidence of a somewhat warmer and wetter climate during MIS4 than during MIS3. Comparison of the two paleosols from other localities is needed to confirm what appears to be the degree of difference in weathering or pedogenesis or both. The unnamed paleosol is a composite paleosol because it is welded to the Sangamon paleosol that developed in the underlying Loveland Loess. The 2At and 2ABt horizons of the unnamed paleosol total 55 cm and are slightly higher in clay (about 2 percent) and sand (about 2 percent) than the Roxana Silt above the paleosol. These small differences indicate formation on an active surface with incorporation of clay and sand from local sources. The degree and extent of soil development was influenced by the climate and time of exposure before burial by the remainder of the Roxana Silt.

- Based on pedostratigraphic and age data, Markewich and others (1998b) suggested that in the tri-State area of southwestern Tennessee, northwestern Mississippi, and east-central Arkansas (fig. 1*A*), there was a several-thousand-year period in early MIS3 (table 1) during which the rate of Roxana Silt deposition was somewhat greater than the rates of weathering and pedogenic alteration. This interval of greater loess deposition rates appears to have occurred after development of the unnamed paleosol. Whether this period represents a period of Laurentide Ice Sheet advance and retreat from the upper Mississippi Valley is beyond the scope of this report. The reader is referred to Kerr and others (2021) for evidence of two MIS3 Laurentide Ice Sheet advances into Iowa that possibly served as the source of the Roxana Silt during this interval.

- Markewich and others (2011) discussed down-valley changes in lower Mississippi Valley MIS5–early MIS2 pedostratigraphy from southern Illinois to west-central Mississippi. They documented a down-valley increase in precipitation and temperature during Sangamon paleosol development during MIS5 through early MIS4. They also observed a down-valley decrease in Roxana Silt thickness, and an increase in the thickness of a mixing zone composed of Roxana Silt, older loess and paleosols, and colluvium in the stratigraphic position of the Roxana Silt. Their observations supported the observations of Miller and Alford (1985) and Alford and Miller (1985) that the Roxana Silt is not present south of about Tchula, Mississippi (fig. 1*B*). To date, paleosol/loess stratigraphy in the lower Mississippi Valley south of Tchula is not resolved; however, recognizing and interpreting down-valley stratigraphic changes are vital to our understanding of lower Mississippi Valley paleoclimates in the late Pleistocene. More investigations of late MIS5–MIS2 deposits in the lower Mississippi Valley from northern Mississippi to Louisiana could greatly augment our understanding of the spatial and temporal dynamics of climate change in the southernmost lower Mississippi Valley during the transitional period from full interglacial (early MIS5) to full glacial (MIS2) conditions. Detailed chronostratigraphic data, pedostratigraphic descriptions, chemical analyses, and SEM/EDS analysis to document down-valley changes in weathering and pedogenesis for each stratigraphic unit could strengthen future studies. Muhs and others (2001) documented down-valley trends in the modern postglacial soil developed in the Peoria Loess from northern Iowa to Louisiana. Markewich and others (2011) documented similar trends in the Sangamon paleosol developed in the Loveland Loess from southern Illinois to west central Mississippi. No such studies document down-valley changes in the Roxana Silt and its associated paleosols.

- Since the 1980s, many studies have addressed the spatial and temporal relations of either loess deposition or paleosol development or both in the Mississippi Valley to Laurentide Ice Sheet advance and retreat (Winters and others, 1988; Forman and others, 1992; Clark and

others, 1993; Leigh, 1994; Curry and Pavich, 1996; Forman and Pierson, 2002; Rittenour and others, 2007; Wang and others, 2009; Pigati and others, 2015; Muhs and others, 2018; Kerr and others, 2021, and references in these articles). The spatial and temporal dynamics of the Laurentide Ice Sheet from late MIS5–MIS3 have been the subject of modeling efforts (Dalton and others, 2019, 2022, and references in these articles). These modeled reconstructions by Dalton and others (2019, 2022) of Laurentide Ice Sheet advances and retreats in the Mississippi Valley suggested that: (1) there were multiple periods of ice-sheet growth and recession from 115–80 ka (middle and late MIS5); (2) by about 60 ka (MIS4), the ice sheet had advanced almost to its last glacial maximum extent (about 25 ka, MIS2) (fig. 1*A*); (3) by about 45 ka (MIS3), the ice sheet had retreated from the upper Mississippi Valley; and (4) by about 35 ka (late MIS3), the ice sheet was expanding rapidly into the upper Mississippi Valley, reaching its maximum at about 25 ka (MIS2). The results of these investigations by Dalton and others (2019, 2022) generally agree with paleoclimate interpretations for the transitional climate of lower Mississippi Valley from late MIS5–MIS2.

References Cited

Alford, J.J., and Miller, B.J., 1985, Loesses in the Lower Mississippi Valley—I. A multiple component model for their deposition and distribution [abs.]. Madison, Wis., American Society of Agronomy Abstracts, p. 188.

Busacca, A.J., Begét, J.E., Markewich, H.W., Muhs, D.R., Lancaster, N., and Sweeney, M.R., 2003, Eolian sediments: Developments in Quaternary Sciences, v. 1, p. 275–309, accessed July 17, 2022, at https://doi.org/10.1016/S1571-0866(03)01013-3.

Clark, P.U., Clague, J.J., Curry, B.B., Dreimanis, A., Hicock, S.R., Miller, G.H., Berger, G.W., Eyles, N., Lamothe, M., Miller, B.B., Mott, R.J., Oldale, R.N., Stea, R.R., Szabo, J.P., Thorleifson, L.H., and Vincent, J.-S., 1993, Initiation and development of the Laurentide and Cordilleran Ice Sheets following the last interglaciation: Quaternary Science Reviews, v. 12, no. 2, p. 79–114, accessed October 25, 2022, at https://doi.org/10.1016/0277-3791(93)90011-A.

Clark, P.U., Nelson, A.R., McCoy, W.D., Miller, B.B., and Barnes, D.K., 1989, Quaternary aminostratigraphy of Mississippi Valley loess: Geological Society of America Bulletin, v. 101, no. 7, p. 918–926, accessed October 24, 2022, at https://doi.org/10.1130/0016-7606(1989)101<0918:QAOMVL>2.3.CO;2.

Curry, B.B., and Pavich, M.J., 1996, Absence of glaciation in Illinois during marine isotope stages 3 through 5: Quaternary Research, v. 46, no. 1, p. 19–26, accessed May 20, 2022, at https://doi.org/10.1006/qres.1996.0040.

Dalton, A.S., Finkelstein, S.A., Forman, S.L., Barnett, P.J., Pico, T., and Mitrovica, J.X., 2019, Was the Laurentide Ice Sheet significantly reduced during Marine Isotope Stage 3?: Geology, v. 47, no. 2, p. 111–114, accessed July 2, 2022, at https://doi.org/10.1130/G45335.1.

Dalton, A.S., Stokes, C.R., and Batchelor, C.L., 2022, Evolution of the Laurentide and Innuitian ice sheets prior to the Last Glacial Maximum (115 ka to 25 ka): Earth-Science Reviews, v. 224, article 103875, accessed June 30, 2022, at https://doi.org/10.1016/j.earscirev.2021.103875.

Dixon, J.B., and White, G.N., 1993, Soil mineralogy electron microscopy workshop: College Station, Tex., published by the authors, Department of Soil and Crop Science, Texas A&M University, 57 p.

Dixon, J.B., and White, G.N., 1999, Soil mineralogy laboratory manual (5th ed.): College Station, Tex., published by the authors, Department of Soil and Crop Science, Texas A&M University, 139 p.

Follmer, L.R., 1996, Loess studies in the central United States—evolution of concepts: Engineering Geology, v. 45, no. 1–4, p. 287–304, accessed May 17, 2022, at https://doi.org/10.1016/S0013-7952(96)00018-X.

Forman, S.L., 1989, Applications and limitations of thermoluminescence to date Quaternary sediments: Quaternary International, v. 1, p. 47–59, accessed October 23, 2022, at https://doi.org/10.1016/1040-6182(89)90008-6.

Forman, S.L., Bettis, E.A., III, Kemmis, T.J., and Miller, B.B., 1992, Chronologic evidence for multiple periods of loess deposition during the late Pleistocene in the Missouri and Mississippi River Valley, United States—Implications for the activity of the Laurentide ice sheet: Palaeogeography, Palaeoclimatology, Palaeoecology, v. 93, no. 1–2, p. 71–83, accessed October 25, 2022, at https://doi.org/10.1016/0031-0182(92)90184-7.

Forman, S.L., and Pierson, J., 2002, Late Pleistocene luminescence chronology of loess deposition in the Missouri and Mississippi river valleys, United States: Palaeogeography, Palaeoclimatology, Palaeoecology, v. 186, no. 1–2, p. 25–46, accessed July 2, 2022, at https://doi.org/10.1016/S0031-0182(02)00440-6.

Grimley, D.A., Larsen, D., Kaplan, S.W., Yansa, C.H., Curry, B.B., and Oches, E.A., 2009, A multi-proxy palaeoecological and palaeoclimatic record within full glacial lacustrine deposits, western Tennessee, USA: Journal of Quaternary Science, v. 24, no. 8, p. 960–981, accessed April 26, 2022, at https://doi.org/10.1002/jqs.1275.

Guccione, M.J., and Rutledge, E.M., 1990, Field guide to the Mississippi alluvial valley, northeast Arkansas and southeast Missouri—Friends of the Pleistocene South-Central Cell, March 30–April 1, 1990: Fayetteville, Ark., Department of Geology, University of Arkansas, 345 p.

Huntley, D.J., Godfrey-Smith, D.I., and Thewalt, M.L.W., 1985, Optical dating of sediments: Nature, v. 313, no. 5998, p. 105–107, accessed October 23, 2022, at https://doi.org/10.1038/313105a0.

Immonen, N., 2013, Surface microtextures of ice-rafted quartz grains revealing glacial ice in the Cenozoic Arctic: Palaeogeography, Palaeoclimatology, Palaeoecology, v. 374, p. 293–302, accessed November 12, 2022, at https://doi.org/10.1016/j.palaeo.2013.02.003.

Jacobs, P.M., and Knox, J.C., 1994, Provenance and pedology of a long-term Pleistocene depositional sequence in Wisconsin's Driftless Area: Catena, v. 22, p. 49–68, accessed March 30, 2023, at https://doi.org/10.1016/0341-8162(94)90065-5.

Jacobs, P.M., Konen, M.E., and Curry, B.B., 2009, Pedogenesis of a catena of the Farmdale–Sangamon Geosol complex in the north central United States: Palaeogeography, Palaeoclimatology, Palaeoecology, v. 282, no 1–4, p. 119–132, accessed March 30, 2023, at https://doi.org/10.1016/j.palaeo.2009.08.017.

Kerr, P.J., Tassier-Surine, S.A., Kilgore, S.M., Bettis, E.A., III, Dorale, J.A., and Cramer, B.D., 2021, Timing, provenance, and implications of two MIS 3 advances of the Laurentide Ice Sheet into the Upper Mississippi River Basin, USA: Quaternary Science Reviews, v. 261, p. 106926, accessed August 29, 2022, at https://doi.org/10.1016/j.quascirev.2021.106926.

Krinsley, D.H., and Doornkamp, J.C., 1973, Atlas of quartz sand surface textures: London, Cambridge University Press, 91 p.

Leigh, D.S., 1994, Roxana Silt of the Upper Mississippi Valley—Lithology, source, and paleoenvironment: Geological Society of America Bulletin, v. 106, no. 3, p. 430–442, accessed July 21, 2022, at https://doi.org/10.1130/0016-7606(1994)106<0430:RSOTUM>2.3.CO;2.

Leigh, D.S., and Knox, J.C., 1994, Loess of the Upper Mississippi Valley driftless area: Quaternary Research, v. 42, no. 1, p. 30-40.

Lyell, C., 1847, On the delta and alluvial deposits of the Mississippi and other points in the geology of North America: American Journal of Science and the Arts, v. 3, no. 2, p. 34–37.

Mahaney, W.C., 2002, Atlas of sand grain surface textures and applications: New York, Oxford University Press, 237 p.

Markewich, H.W., Pavich, M.J., and Wysocki, D.A., 1998a, Stage 3 Climate/loess relations in the Lower Mississippi Valley, U.S.A., *in* Busacca, A., ed., Dust aerosols, loess soils, and global change: an interdisciplinary conference and field tour on dust in ancient environments and contemporary environmental management, October 11–13, 1998, Seattle, Washington: Washington State University, College of Agriculture and Home Economics Miscellaneous Publication No. MISV0190, p. 159–162.

Markewich, H.W., Pavich, M.J., Wysocki, D.A., White, G.N., and Dixon, J.B., 2010, The enigmatic Roxana Silt [abs.]: Geological Society of America Abstracts with Programs, v. 42, no. 5, p. 73, accessed August 11, 2022, at https://gsa.confex.com/gsa/2010AM/webprogram/Paper178488.html.

Markewich, H.W., Wysocki, D.A., Pavich, M.J., and Rutledge, E.M., 2011, Age, genesis, and paleoclimatic interpretation of the Sangamon/Loveland complex in the Lower Mississippi Valley, U.S.A.: Geological Society of America Bulletin, v. 123, no. 1–2, p. 21–39, accessed May 11, 2022, at https://doi.org/10.1130/B30208.1.

Markewich, H.W., Wysocki, D.A., Pavich, M.J., Rutledge, E.M., Millard, H.T., Jr., Rich, F.J., Maat, P.B., Rubin, M., and McGeehin, J.P., 1998b, Paleopedology plus TL, ^{10}Be, and ^{14}C dating as tools in stratigraphic and paleoclimatic investigations, Mississippi River Valley, U.S.A.: Quaternary International, v. 51–52, p. 143–167, accessed May 29, 2022, at https://doi.org/10.1016/S1040-6182(97)00041-4.

McCoy, W.D., Oches, E.A., and Clark, P.U., 1990, Results of aminostratigraphic investigations at Wittsburg, Crowley's Ridge, Arkansas, *in* Guccione, M.J., and Rutledge, E.M., eds., Field guide to the Mississippi alluvial valley, northeast Arkansas and southeast Missouri—Friends of the Pleistocene South-Central Cell, March 30–April 1, 1990: Fayetteville, Ark., Department of Geology, University of Arkansas, p. 99–101.

McCraw, D.J., and Autin, W.J., 1989, A review of historic and modern concepts of Lower Mississippi Valley loess stratigraphy, *in* Lower Mississippi Valley loess field guide—The Mississippi Valley loess tour 1989—organized by INQUA Commission on Loess and the North American Loess Working Group, Leon Follmer, coordinator: Baton Rouge, La., Louisiana Geological Survey, 35 p., accessed March 22, 2023, at https://www.scribd.com/document/18935222/1989-Louisiana-Loess-Fieldtrip-Guidebook.

Millard, H.T., Jr., and Maat, P.B., 1994, Thermoluminescence dating procedures in use at the U.S. Geological Survey, Denver, Colorado: U.S. Geological Survey Open-File Report 94–249, p. 23, accessed May 12, 2022, at https://doi.org/10.3133/ofr94249.

Miller, B.B., McCoy, W.D., and Johnson, W.H., 1988, Aminostratigraphy of pre-Wisconsin deposits in Illinois [abs.]: Geological Society of America Abstracts with Programs, v. 20, p. A345.

Miller, B.J., and Alford, J.J., 1985, Loesses in the Lower Mississippi Valley—II. Correlation and distribution with respect to Upper Mississippi Valley loesses [abs.]: Madison, Wis., American Society of Agronomy Abstracts, p. 196.

Miller, B.J., Lewis, G.C., Alford, J.J., and Day, W.J., 1985, Loesses in Louisiana and at Vicksburg, Mississippi: Field trip guidebook for Southeastern Friends of the Pleistocene Annual Meeting, April 12, 13, and 14, 1984: Baton Rouge, La., Louisiana State University Agricultural Center, 126 p.

Mirecki, J.E., and Miller, B.B., 1994, Aminostratigraphic correlation and geochronology of two Quaternary loess localities, central Mississippi Valley: Quaternary Research, v. 41, no. 3, p. 289–297, accessed October 24, 2022, at https://doi.org/10.1006/qres.1994.1033.

Mirecki, J., and Skinner, A., 1991, Aminostratigraphy and electron spin resonance dating of terrestrial mollusks from late Quaternary loesses of the central Mississippi Valley [abs.]: Geological Society of America Abstracts with Programs, v. 23, no. 5, p. A408.

Muhs, D.R., Bettis, E.A., III, Been, J., and McGeehin, J.P., 2001, Impact of climate and parent material on chemical weathering in loess-derived soils of the Mississippi River Valley: Soil Science Society of America Journal, v. 65, no. 6, p. 1761–1777, accessed November 13, 2022, at https://doi.org/10.2136/sssaj2001.1761.

Muhs, D.R., Bettis, E.A., III, and Skipp, G.L., 2018, Geochemistry and mineralogy of late Quaternary loess in the upper Mississippi River valley, USA—Provenance and correlation with Laurentide Ice Sheet history: Quaternary Science Reviews, v. 187, p. 235–269, accessed October 14, 2022, at https://doi.org/10.1016/j.quascirev.2018.03.024.

Munsell Color Company, 1992, Munsell soil color charts revised edition: New York and Baltimore, Munsell Color, Macbeth—Division of Kollmorgen Instruments Corp. [leaves, unpaged].

National Cooperative Soil Survey, [undated], National Cooperative Soil Survey (NCSS) soil characterization database: NCSS database, accessed May 23, 2022, at https://ncsslabdatamart.sc.egov.usda.gov/. [NCSS soil characterization basic query; User Pedon ID S1992AR107002.]

Pavich, M.J., 1993, Dating techniques, beryllium-10, *in* Markewich, H.W., ed., Progress report on chronostratigraphic and paleoclimate studies, middle Mississippi River Valley, eastern Arkansas and western Tennessee: U.S. Geological Survey Open-File Report 93–273, p. 7–8, accessed May 11, 2022, at https://doi.org/10.3133/ofr93273.

Pavich, M.J., Brown, L., Klein, J., and Middleton, R., 1984, ^{10}Be accumulation in a soil chronosequence: Earth and Planetary Science Letters, v. 68, no. 2, p. 198–204, accessed October 23, 2022, at https://doi.org/10.1016/0012-821X(84)90151-1.

Pavich, M.J., and Markewich, H.W., 1994, Beryllium-10 (Be-10), *in* Markewich, H.W., ed., Second progress report on chronostratigraphic and paleoclimate studies, middle Mississippi River Valley, eastern Arkansas and western Tennessee: U.S. Geological Survey Open-File Report 94–208, p. 6.

Pigati, J.S., McGeehin, J.P., Muhs, D.R., Grimley, D.C., and Nekola, J.C., 2015, Radiocarbon dating loess deposits in the Mississippi Valley using terrestrial gastropod shells (Polygyridae, Helicinidae, Discidae): Aeolian Research, v. 16, p. 25–33, accessed November 13, 2022, at https://doi.org/10.1016/j.aeolia.2014.10.005.

Pye, K., and Johnson, R., 1988, Stratigraphy, geochemistry, and thermoluminescence ages of lower Mississippi Valley loess: Earth Surface Processes and Landforms, v. 13, no. 2, p. 103–124, accessed October 25, 2022, at https://doi.org/10.1002/esp.3290130203.

Railsback, L.B., Gibbard, P.L., Head, M.J., Voarintsoa, N.R.G., and Toucanne, S., 2015, An optimized scheme of lettered marine isotope substages for the last 1.0 million years, and the climatostratigraphic nature of isotope stages and substages: Quaternary Science Reviews, v. 111, p. 94–106, accessed November 12, 2020, at https://doi.org/10.1016/j.quascirev.2015.01.012.

Rittenour, T.M., Blum, M.D., and Goble, R.J., 2007, Fluvial evolution of the lower Mississippi River Valley during the last 100 k.y. glacial cycle—Response to glaciation and sea-level change: Geological Society of America Bulletin, v. 119, no. 5–6, p. 586–608, accessed July 17, 2022, at https://doi.org/10.1130/B25934.1.

Rodbell, D.T., Forman, S.L., Pierson, J., and Lynn, W.C., 1997, Stratigraphy and chronology of Mississippi Valley loess in western Tennessee: Geological Society of America Bulletin, v. 109, no. 9, p. 1134–1148, accessed May 30, 2022, at https://doi.org/10.1130/0016-7606(1997)109<1134:SACOMV>2.3.CO;2.

Rubin, M., McGeehin, J.P., and Markewich, H.W., 1993, Dating techniques, carbon-14, *in* Markewich, H.W., ed., Progress report on chronostratigraphic and paleoclimate studies, middle Mississippi River Valley, eastern Arkansas and western Tennessee: U.S. Geological Survey Open-File Report 93–273, p. 6–7, accessed May 11, 2022, at https://doi.org/10.3133/ofr93273.

Rutledge, E.M., Guccione, M.J., Markewich, H.W., Wysocki, D.A., and Ward, L.B., 1996, Loess stratigraphy of the Lower Mississippi Valley: Engineering Geology, v. 45, no. 1–4, p. 167–183, accessed May 17, 2022, at https://doi.org/10.1016/S0013-7952(96)00012-9.

Rutledge, E.M., West, L.T., and Guccione, M.J., 1990, Loess deposits of northeast Arkansas, *in* Guccione, M.J., and Rutledge, E.M., eds., Field guide to the Mississippi alluvial valley, northeast Arkansas and southeast Missouri—Friends of the Pleistocene South-Central Cell, March 30–April 1, 1990: Fayetteville, Ark., Department of Geology, University of Arkansas, p. 57–78.

Saucier, R.T., 1994, Geomorphology and Quaternary geologic history of the lower Mississippi Valley: Vicksburg, Miss., U.S. Army Corps of Engineers Waterways Experiment Station, 364 p.

Schoeneberger, P.J., Wysocki, D.A., Benham, E.C., and Broderson, W.D., 1998, Field book for describing and sampling soils, version 1.1: Lincoln, Nebr., Natural Resources Conservation Service, National Soil Survey Center [leaves, unnumbered].

Skinner, A.F., and Mirecki, J., 1993, ESR dating of molluscs—Is it only a "shell game"?: Applied Radiation and Isotopes, v. 44, no. 1–2, p. 139–143, accessed July 3, 2022, at https://doi.org/10.1016/0969-8043(93)90208-R.

Soil Survey Division Staff, 1993, Soil Survey Manual, 2nd edition, U.S. Department of Agriculture Handbook no. 18, 437 p., accessed March 29, 2023, at https://books.google.com/books?id=LYwwAAAAYAAJ&printsec=frontcover&source=gbs_ge_summary_r&cad=0#v=onepage&q&f=false.

Soil Survey Staff, 1975, Soil taxonomy, a basic system of soil classification for making and interpreting soil surveys: United States Department of Agriculture Natural Resources Conservation Service Agriculture Handbook No. 436, 754 p.

Soil Survey Staff, 1999, Soil taxonomy, a basic system of soil classification for making and interpreting soil surveys (2d ed.): United States Department of Agriculture Natural Resources Conservation Service Agriculture Handbook No. 436, 886 p., accessed November 15, 2022, at https://www.nrcs.usda.gov/sites/default/files/2022-06/Soil%20Taxonomy.pdf.

Soil Survey Staff, 2014, Kellogg Soil Survey Laboratory methods manual (version 5.0): Burt, R., and Soil Survey Staff, eds., U.S. Department of Agriculture, Natural Resources Conservation Service, Soil Survey Investigations Report No. 42, 1,031 p., accessed April 4, 2023, at https://data.neonscience.org/documents/10179/2357445/KelloggSSL_MethodsManual_Report42Version5_2014/da9589dd-3278-402b-a5d4-02dc0c9c762c.

Thorp, J., Smith, H.T.U., Baldwin, M., Bowser, W.E., Flint, R.F., Gould, L.M., Moss, H.C., Reed, E.C., Smith, G.D., and Trowbridge, A.C., 1952, Pleistocene eolian deposits of the United States, Alaska, and parts of Canada: National Research Council Committee for the Study of Eolian Deposits, Geological Society of America Map, scale 1:2,500,000.

Wang, H., Lundstrom, C.C., Zhang, Z., Grimley, D.A., and Balsam, W.L., 2009, A mid–late Quaternary loess–paleosol record in Simmons Farm in southern Illinois, USA: Quaternary Science Reviews, v. 28, no. 1–2, p. 93–106, accessed August 10, 2022, at https://doi.org/10.1016/j.quascirev.2008.09.021.

Ward, L.B., Rutledge, E.M., and Wysocki, D.A., 1993, Detailed loess and paleosol stratigraphy, *in* Markewich, H.W., ed., Progress report on chronostratigraphic and paleoclimate studies, middle Mississippi River Valley, eastern Arkansas and western Tennessee: U.S. Geological Survey Open-File Report 93–273, p. 10–23, accessed May 11, 2022, at https://doi.org/10.3133/ofr93273.

White, G.N., 2008, Scanning electron microscopy, *in* Ulery, L. and Drees, R.L., eds., Methods of soil analysis part 5—mineralogical methods: Madison, Wis., Soil Science Society of America Book Series, p. 269–297, accessed May 11, 2022, at https://doi.org/10.2136/sssabookser5.5.c10.

Winters, H.A., Alford, J.J., and Rieck, R.L., 1988, The anomalous Roxana Silt and mid-Wisconsinan events in and near southern Michigan: Quaternary Research, v. 29, no. 1, p. 25–35, accessed August 25, 2022, at https://doi.org/10.1016/0033-5894(88)90068-3.

Woronko, B., and Pisarska-Jamroży, M., 2016, Micro-scale frost weathering of sand-sized quartz grains: Permafrost and Periglacial Processes, v. 27, no. 1, p. 109–122, accessed November 12, 2022, at https://doi.org/10.1002/ppp.1855.

ISSN 2328-0328 (online)
https://doi.org/10.3133/sir20235062